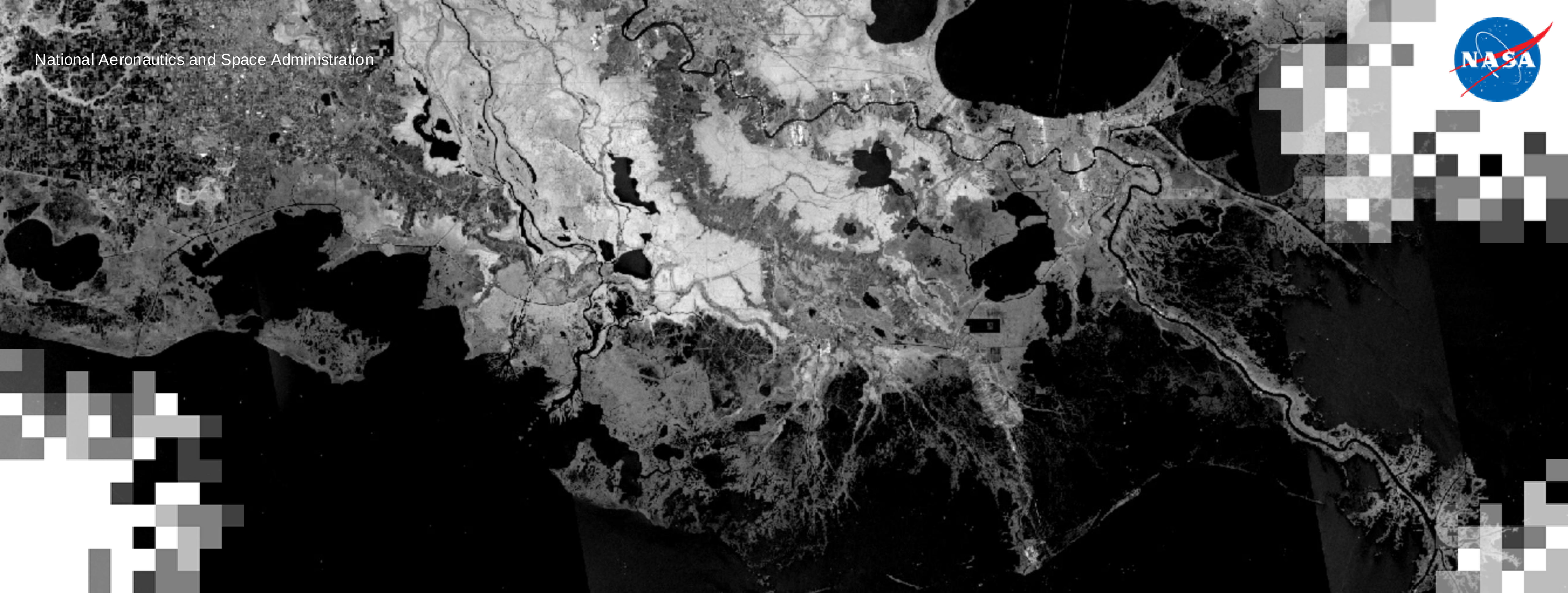

An Introduction to SAR and Its Applications

Part 2: Introduction to Interferometric SAR (InSAR)

Dr. Eric Fielding (JPL)

November 13, 2024

Prior Knowledge

- [ARSET Basics of Synthetic Aperture Radar]
- [ARSET SAR Processing and Data Analysis]

Training Outline

Part 1

Introduction to Synthetic Aperture Radar (SAR)

November 6, 2024

11:30 am - 01:30 pm EST (UTC-5:00)

Part 2

Introduction to Interferometric SAR (InSAR)

November 13, 2024

11:30 am - 01:30 pm EST (UTC-5:00)

Part 3

An Overview of SAR Data Sources and Tools

November 20, 2024

11:30 am - 01:30 pm EST (UTC-5:00)

Homework

Opens November 20 – Due December 4 – Posted on the Training Webpage

A certificate of completion will be awarded to participants who attend all live sessions and complete the homework assignment by the due date.

How to Ask Questions

- Please write your questions in the 'Q&A' window, which you can find in the bottom right under the three '…'. We will address them at the end of this session.
- Feel free to enter your questions during the presentation. We will try to answer all of the questions during the Q&A session at the end of this webinar.
- The remaining questions will be answered in the Q&A document, which will be posted to the training website in approximately one week.

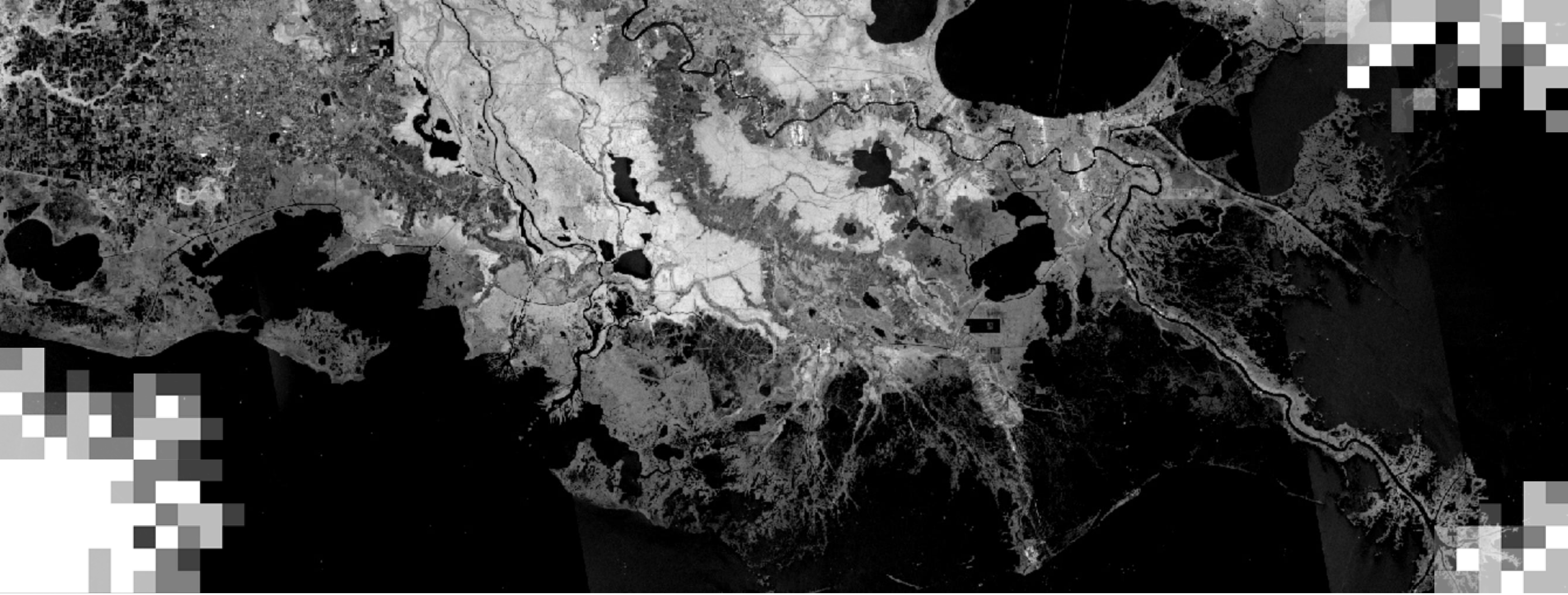

An Introduction to SAR and Its Applications

Part 2: Introduction to Interferometric SAR (InSAR)

Training Learning Objectives

By the end of this session, participants will be able to:

- Identify key concepts of the physics of SAR interferometry
- Recognize what SAR interferometric phase says about the land surface
- Identify the data processing steps to generate a SAR interferogram
- Interpret the information content in SAR interferometric images to measure surface deformation
- Identify application areas in which interferometric SAR is useful

Session 2 – Guest Instructor

Dr. Eric Fielding

Senior Research Scientist

JPL, Caltech

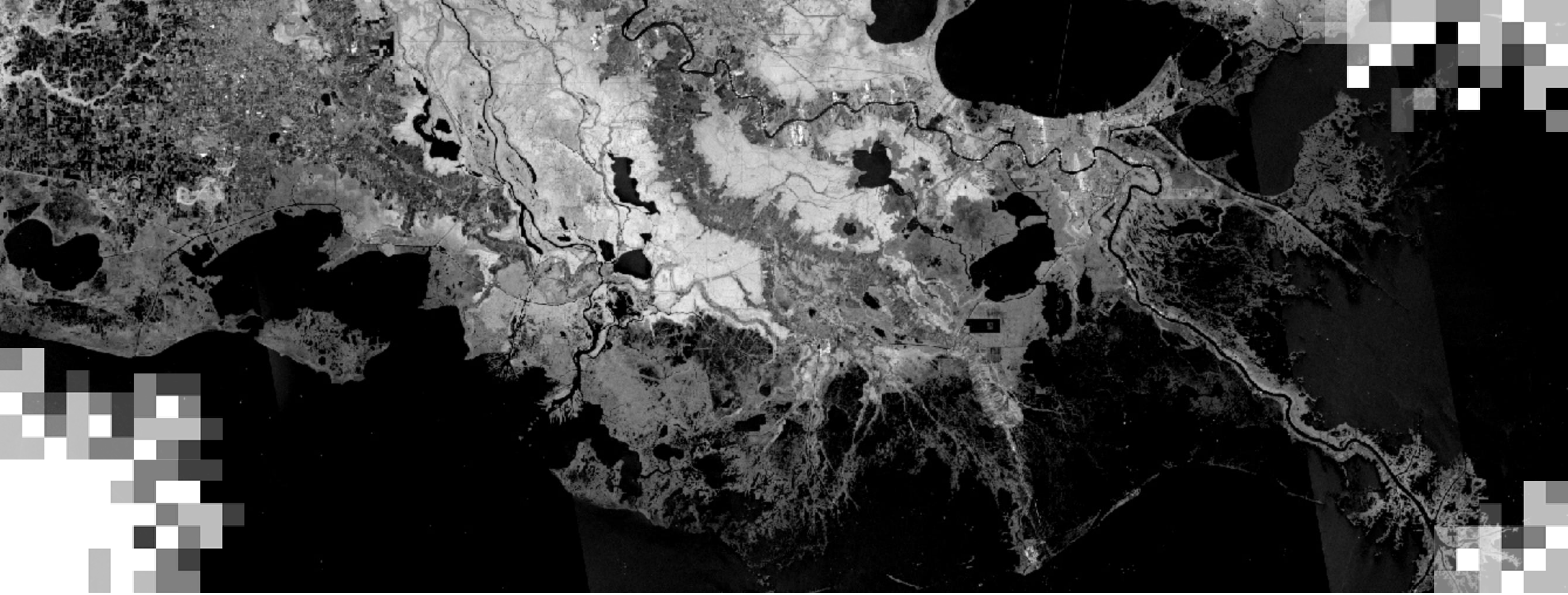

SAR Interferometry Theory

SAR Imagery and Speckle

- Full resolution SAR imagery has a grainy appearance called **speckle**, which is a phenomena due to the coherent nature of SAR imaging.

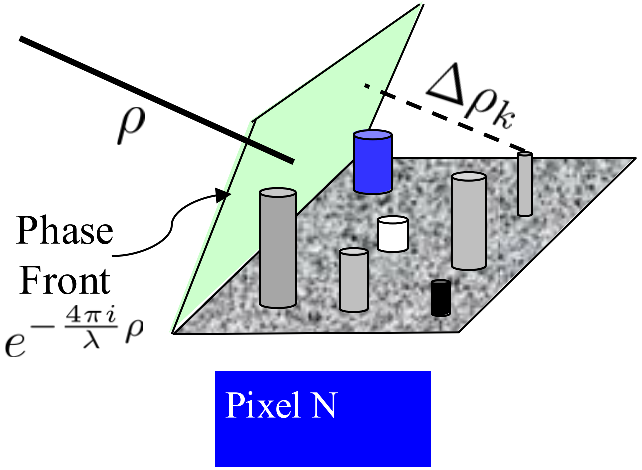

Number and arrangement of scattering elements within resolution cell varies from pixel to pixel.

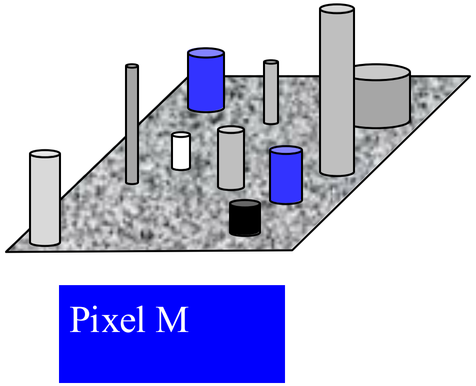

Returned signal is a coherent combination of the returns from the scattering elements.

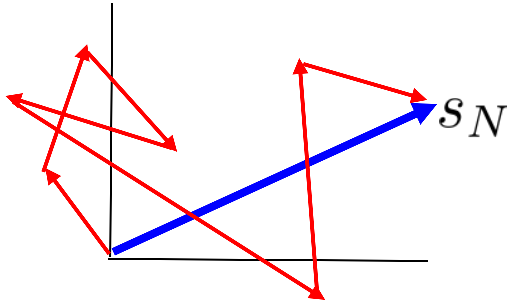

$$s = A \underbrace{e^{-\frac{4\pi i}{\lambda}\rho}}_{\text{Range Phase}} \underbrace{\sum_{k=1}^{N} a_k e^{-\frac{4\pi i}{\lambda}\Delta\rho_k}}_{\text{Scatterer Contribution}}$$

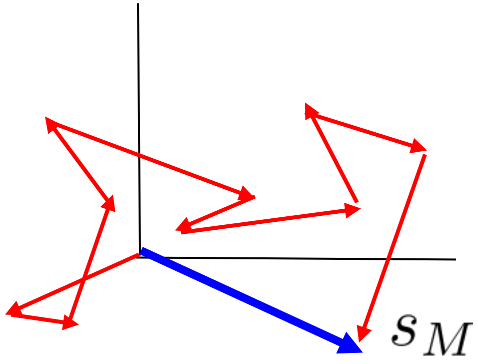

SAR Phase – A Measure of the Range and Surface Complexity

- The phase of the radar signal is the number of **cycles of oscillation** that the wave executes between the radar and the surface and back again.

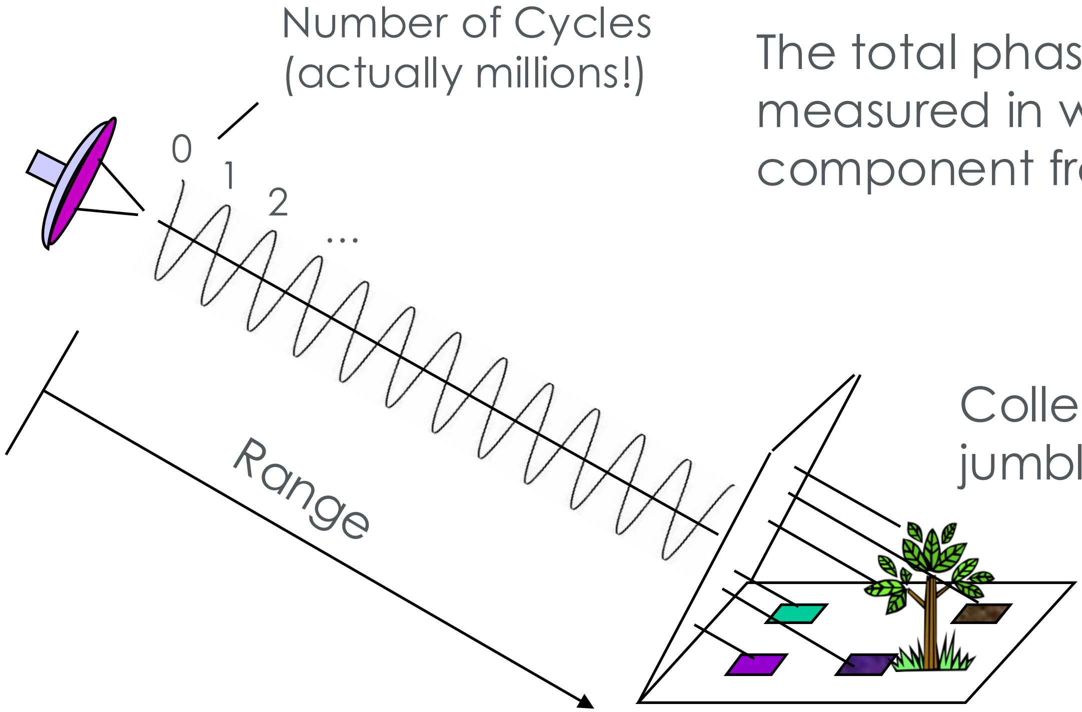

The total phase is two-way range measured in wave cycles + random component from the surface.

Collection of random path lengths jumbles the phase of the echo.

Only **interferometry** can sort it out!

Simplistic View of SAR Phase

Phase of Image 1: $\Phi_1 = \frac{4\pi}{\lambda} \times \rho_1 + other\ constants + \ n_1$

Phase of Image 2: $\Phi_2 = \frac{4\pi}{\lambda} \times \rho_2 + other\ constants + \ n_2$

1. The "other constants" cannot be directly determined.
2. "Other constants" depends on scatterer distribution in the resolution cell, which is unknown and varies from cell to cell.
3. The only way of observing the range change is through interferometry (cancellation of "other constants").

Types of Radar Interferometry

- Two main classes of interferometric radars are separated based on the geometric configuration of the baseline vector:
  - Interferometers are used for topographic measurements when the antennas are separated in the cross-track direction.
  - Interferometers are used to measure line-of-sight motion when the antennas are separated in the along-track direction.
  - A single antenna repeating its path can form an interferometer to measure long-term deformation

Cross-Track Interferometer

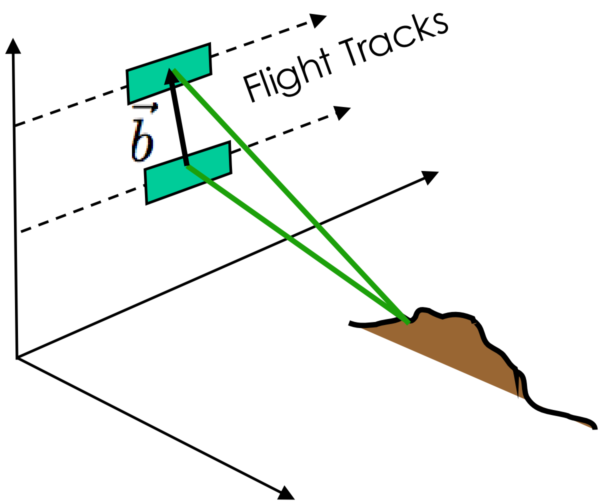

- Dual antenna single pass interferometers
- Single antenna repeat pass interferometers

==> Topography and Deformation

Along-Track Interferometer

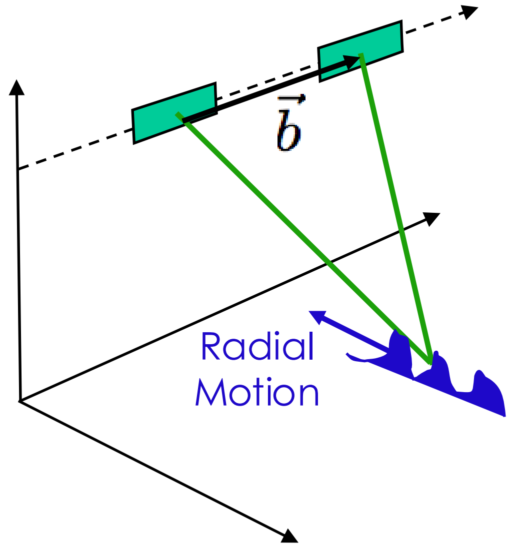

- Dual antenna single pass interferometer
- Along-track separation of milliseconds

==> Radial Velocity

SAR Interferometry Applications: Cartography

- Mapping/Cartography
  - Radar Interferometry from airborne platforms is routinely used to produce topographic maps as digital elevation models (DEMs).
    - 2-5 meter circular position accuracy
    - 5-10 m post spacing and resolution
    - 10 km by 80 km DEMs produced in 1 hr on mini-supercomputer
  - Radar imagery is automatically geocoded, becoming easily combined with other (multispectral) data sets.
  - Applications of topography enabled by interferometric rapid mapping:
    - Land use management, classification, hazard assessment, intelligence, urban planning, short- and long-time scale geology, hydrology

Slide Modified from Paul Rosen (JPL)

SAR Interferometry Applications: Deformation Mapping

- Deformation Mapping and Change Detection
  - Repeat Pass Radar Interferometry from spaceborne platforms is routinely used to produce topographic *change* maps as digital displacement models (DDMs).
    - 0.3-1 centimeter relative displacement accuracy
    - 10-100 m post spacing and resolution
    - 100 km by 100 km DDMs produced rapidly once data is available
  - Applications include:
    - Earthquake and volcano monitoring and modeling, landslides, and subsidence
    - Glacier and ice sheet dynamics
    - Deforestation, change detection, disaster monitoring

Slide Modified from Paul Rosen (JPL)

Interferometry for Topography

Measured Phase Difference:

$$\Delta\phi = -\frac{2\pi}{\lambda}\delta\rho$$

Triangulation:

$$\sin(\theta - a) = \frac{(\rho + \delta\rho)^2 - \rho^2 - B^2}{2\rho B}$$

$$z = h - \rho cos\theta$$

Critical Interferometer Knowledge:
- Baseline, (B,α),to mm's
- System phase differences, to deg's

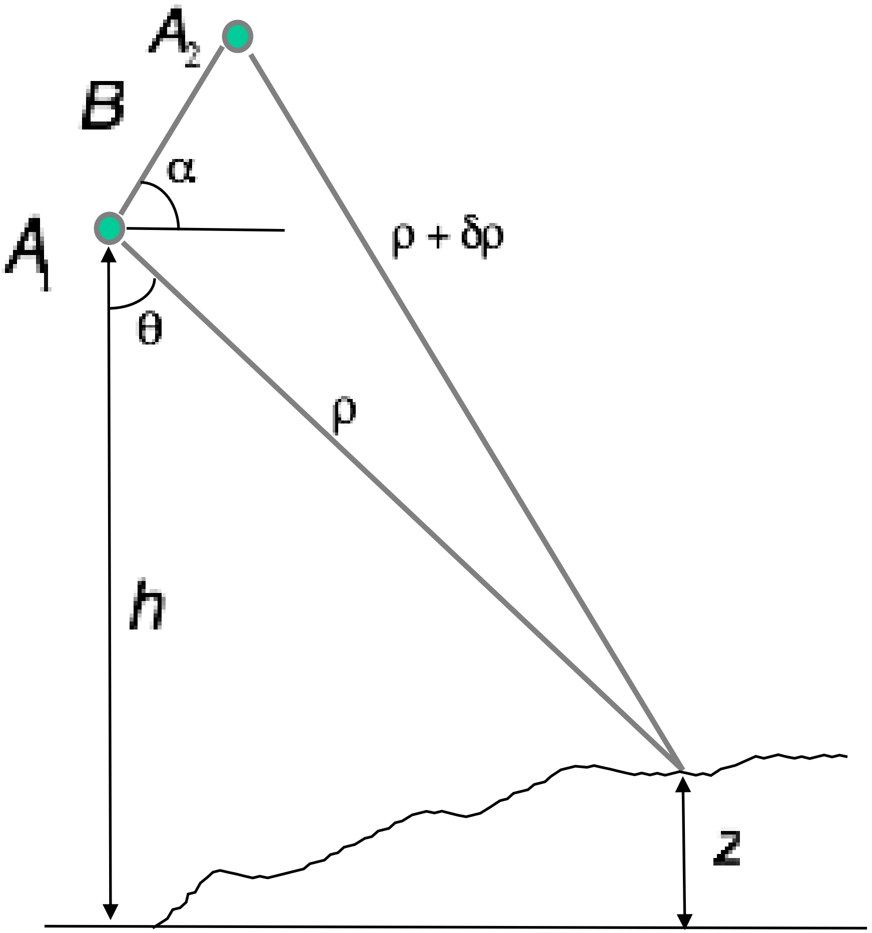

Data Collection Options

For single pass interferometry (SPI) both antennas are located on the same platform, which is ideal for measuring topography. Two modes of data collection are common:

- **Single-Antenna-Transmit Mode –** One antenna transmits and both receive.
- **Ping-Pong Mode –** Each antenna transmits and receives its own echoes, effectively doubling the physical baseline.

Classic

$$\Delta\phi = \frac{2\pi}{\lambda}(\rho_2 + \rho_1) - \frac{2\pi}{\lambda}(\rho_1 + \rho_1)$$

$$= \frac{2\pi}{\lambda}(\rho_2 - \rho_1)$$

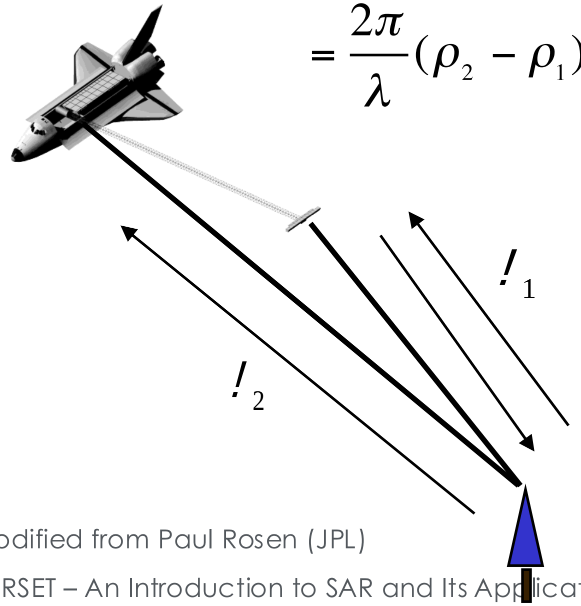

$$\Delta\phi = \frac{2\pi p}{\lambda}\delta\rho,$$

$$p = 1$$

Ping-Pong

$$\Delta\phi = \frac{2\pi}{\lambda}(\rho_2 + \rho_2) - \frac{2\pi}{\lambda}(\rho_1 + \rho_1)$$

$$= \frac{4\pi}{\lambda}(\rho_2 - \rho_1)$$

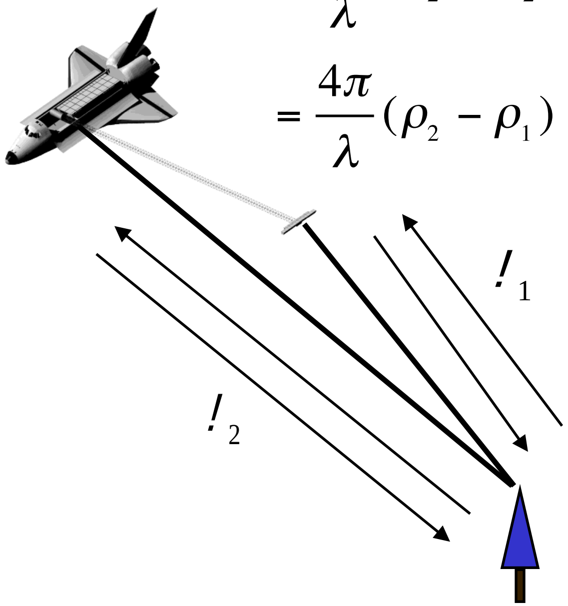

$$\Delta\phi = \frac{2\pi p}{\lambda}\delta\rho,$$

$$p = 2$$

Slide Modified from Paul Rosen (JPL)

Data Collection Options II

Interferometric data can also be collected in the **Repeat Pass Mode (RPI)**. In this mode two spatially close radar observations of the same scene are made separated in time. The time interval may range from seconds to years. The two observations may be made with different sensors provided they have nearly identical radar system parameters. This kind of data can be used for topography or surface deformation measurements.

Second observation made at some later time.

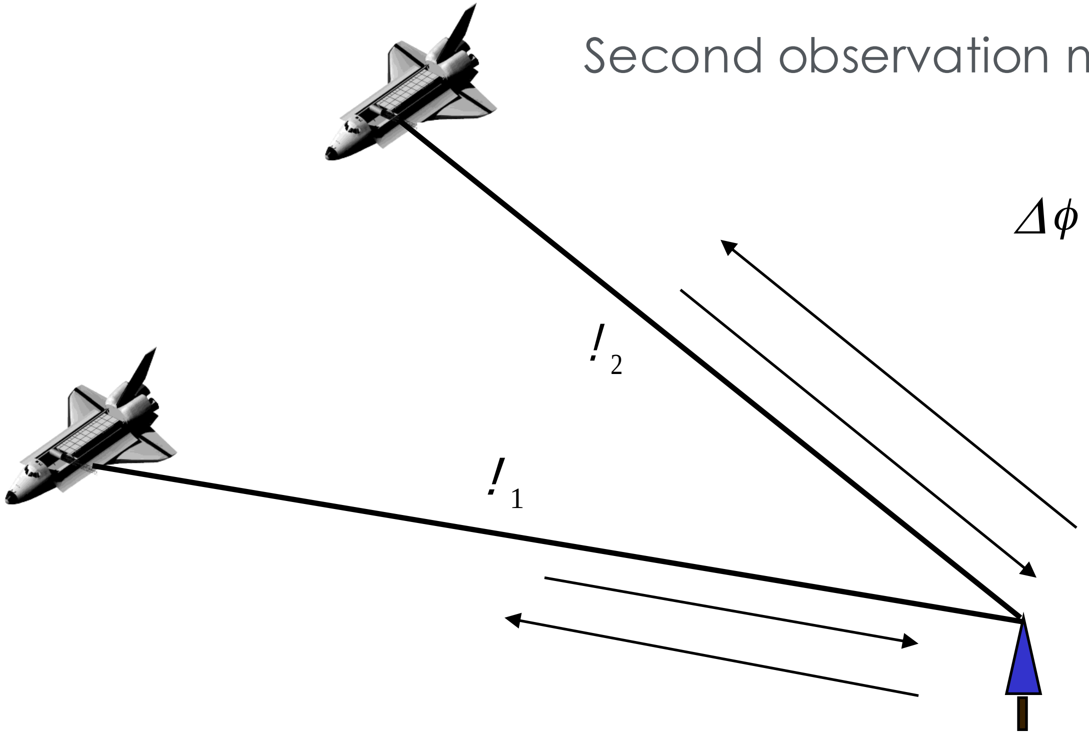

$$\Delta\phi = \frac{2\pi}{\lambda}(\rho_2 + \rho_2) - \frac{2\pi}{\lambda}(\rho_1 + \rho_1)$$

$$= \frac{4\pi}{\lambda}(\rho_2 - \rho_1)$$

$$\Delta\phi = \frac{2\pi p}{\lambda}\delta\rho,$$

$$p = 2$$

Differential Interferometry

When two observations are made from the same location in space but at different times, the interferometric phase is proportional to any change in the range of a surface feature directly.

$$\Delta\phi = \frac{4\pi}{\lambda}\left(\rho(t_1) - \rho(t_2)\right) = \frac{4\pi}{\lambda}\Delta\rho_{\text{change}}$$

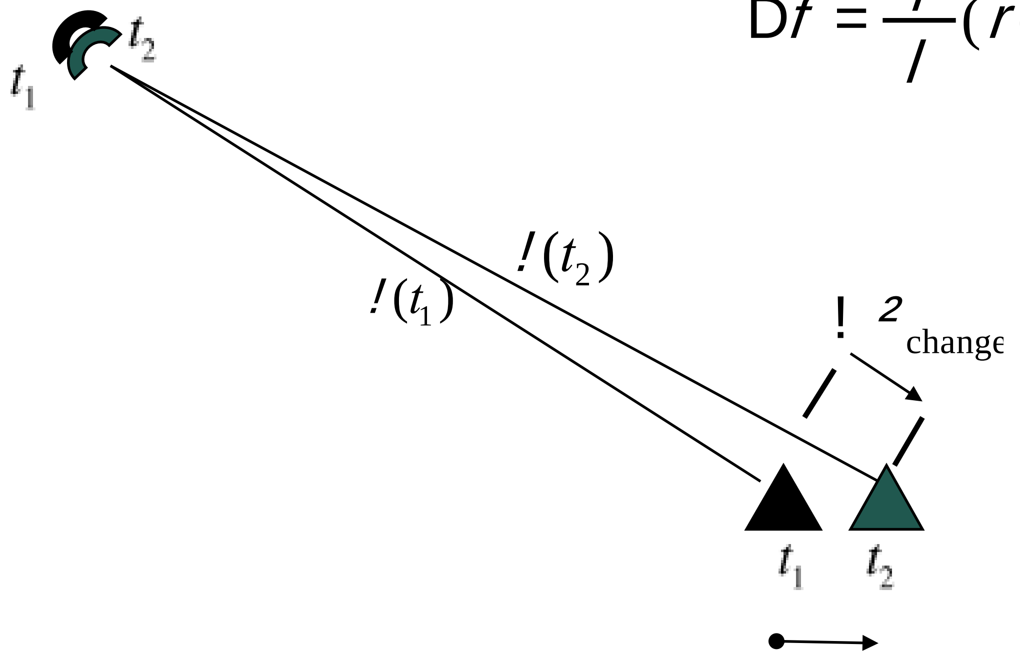

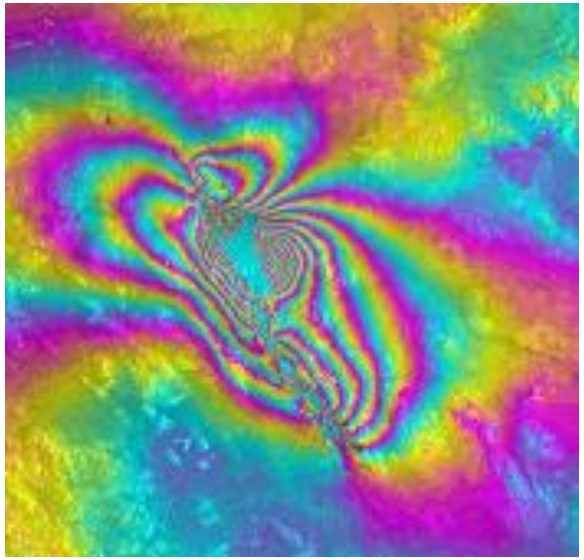

Differential Interferometry and Topography

Generally, two observations are made from different locations in space and at different times, so the interferometric phase is proportional to topography and topographic change.

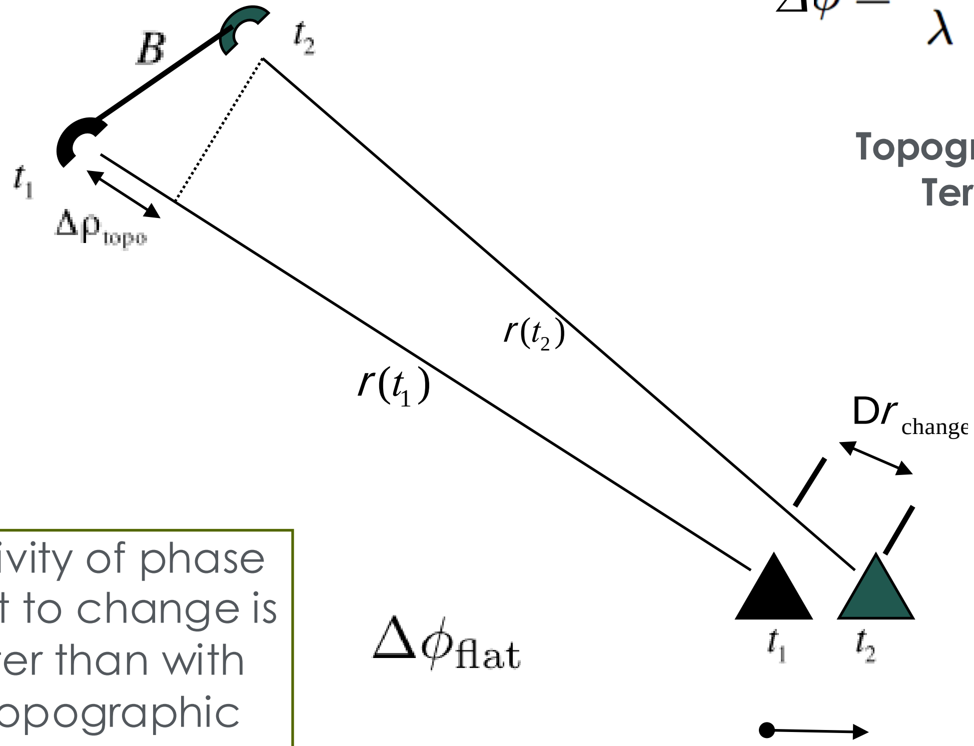

$$\Delta\phi = \frac{4\pi}{\lambda}\left(-\langle\hat{\ell},\vec{b}\rangle + \langle\hat{\ell},\vec{D}\rangle\right)$$

Topography Term ($-\langle\hat{\ell},\vec{b}\rangle$) — **Change Term** ($\langle\hat{\ell},\vec{D}\rangle$)

$$\Delta\phi = \frac{4\pi}{\lambda}(\Delta\rho_{change} - \Delta\rho_{topo})$$

$$\Delta\phi = \frac{4\pi}{\lambda}(\Delta\rho_{change} - b\sin(\theta-\alpha))$$

$$\Delta\phi_{flat} = \frac{4\pi}{\lambda}\left(\Delta\rho_{change} - \frac{b_\perp h_T}{\rho\sin\theta}\right)$$

Note: Sensitivity of phase with respect to change is much greater than with respect to topographic relief.

If topography is known, then second term can be eliminated to reveal surface change.

Differential Interferometry Sensitivities

The reason differential interferometry can detect millimeter-level surface deformation is that the differential phase is much more sensitive to displacements than to topography.

$$\frac{\partial \phi}{\partial h} = \frac{2\pi p b \cos(\theta - \alpha)}{\lambda \rho \sin\theta} = \frac{2\pi p b_\perp}{\lambda \rho \sin\theta}$$

Topographic Sensitivity

$(\phi \Leftrightarrow \Delta\phi)$

$$\frac{\partial \phi}{\partial \Delta\rho} = \frac{4\pi}{\lambda}$$

Displacement Sensitivity

$$\sigma_{\phi_{topo}} = \frac{\partial \phi}{\partial h}\sigma_h = \frac{4\pi}{\lambda}\frac{b_\perp}{\rho \sin\theta}\sigma_h$$

Topographic Sensitivity Term

$$\sigma_{\phi_{disp}} = \frac{\partial \phi}{\partial \Delta\rho}\sigma_{\Delta\rho} = \frac{4\pi}{\lambda}\sigma_{\Delta\rho}$$

Displacement Sensitivity Term

Since: $\frac{b}{\rho} << 1$ ==> $\frac{\sigma_{\phi_{disp}}}{\sigma_{\Delta\rho}} >> \frac{\sigma_{\phi_{topo}}}{\sigma_h}$

Meter-Scale Topography Measurement – Millimeter-Scale Topographic Change

Slide Modified from Paul Rosen (JPL)

Phase Unwrapping

From the measured, wrapped phase, unwrap the phase from some arbitrary starting location, then determine the proper 2π phase "ambiguity".

$$\Delta\phi_{topo} = \frac{2\pi p}{\lambda}(\rho_1 - \rho_2) = \frac{2\pi p}{\lambda}\vec{b}\bullet\vec{l}$$

$$\Delta\phi_{meas} = \text{mod}(\Delta\phi_{topo}, 2\pi)$$

$$\Delta\phi_{unwrap}(s,\rho) = \Delta\phi_{topo}(s,\rho) + \Delta\phi_{const}$$

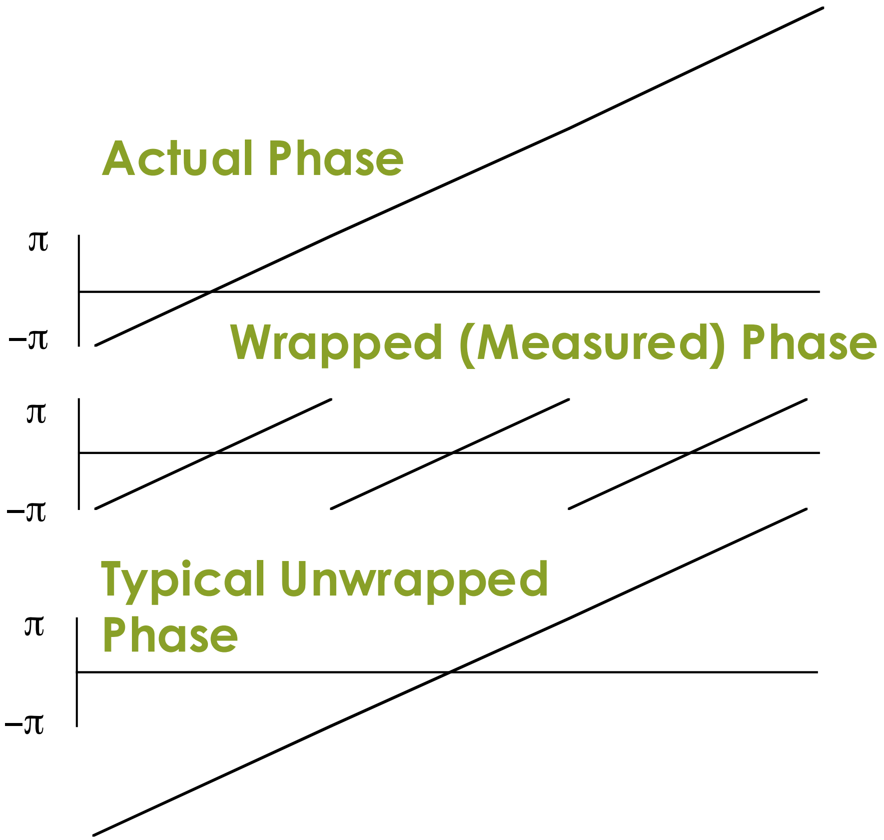

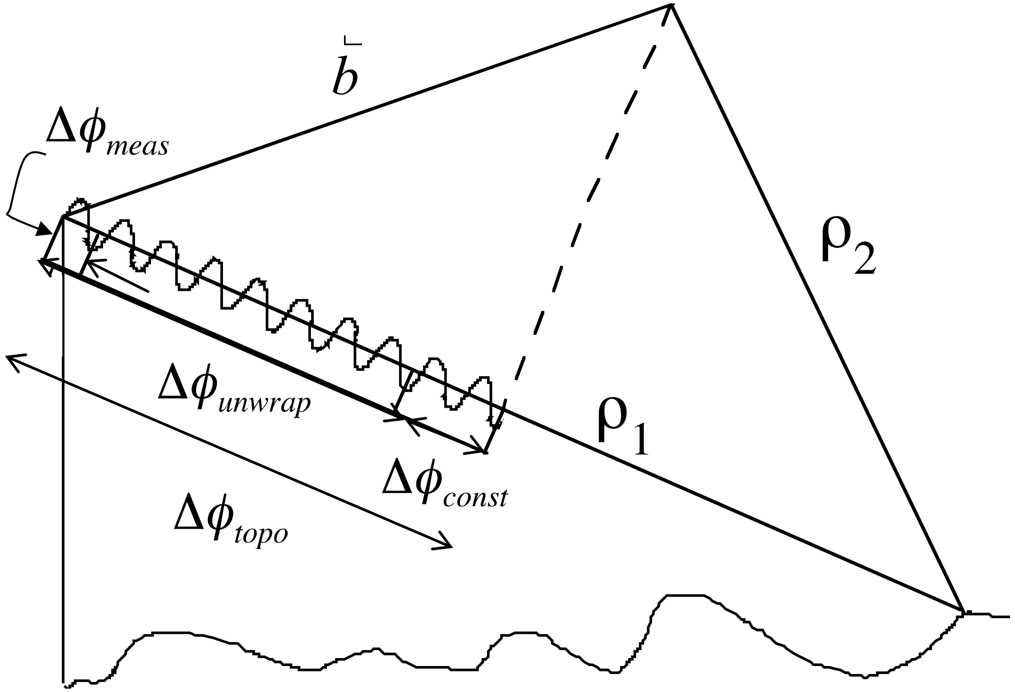

Slide Modified from Paul Rosen (JPL)

Correlation* or Coherence Theory

- InSAR signals decorrelate (become incoherent) due to:
  - Thermal and Processor Noise
  - Differential Geometric and Volumetric Scattering
  - Rotation of Viewing Geometry
  - Random Motions Over Time

- Decorrelation relates to the local phase standard deviation of the interferogram phase.
  - Affects height and displacement accuracy
  - Affects ability to unwrap phase

***"Correlation" and "Coherence" are often used synonymously.**

Slide Modified from Paul Rosen (JPL)

InSAR Correlation Components

- Correlation effects multiply, unlike phase effects that add.
- Low coherence or decorrelation for any reason causes loss of information in that area.

$$\gamma = \gamma_v \gamma_g \gamma_t \gamma_c$$

Where:
γ_v is volumetric (trees)
γ_g is geometric (steep slopes)
γ_t is temporal (gradual changes)
γ_c is sudden changes

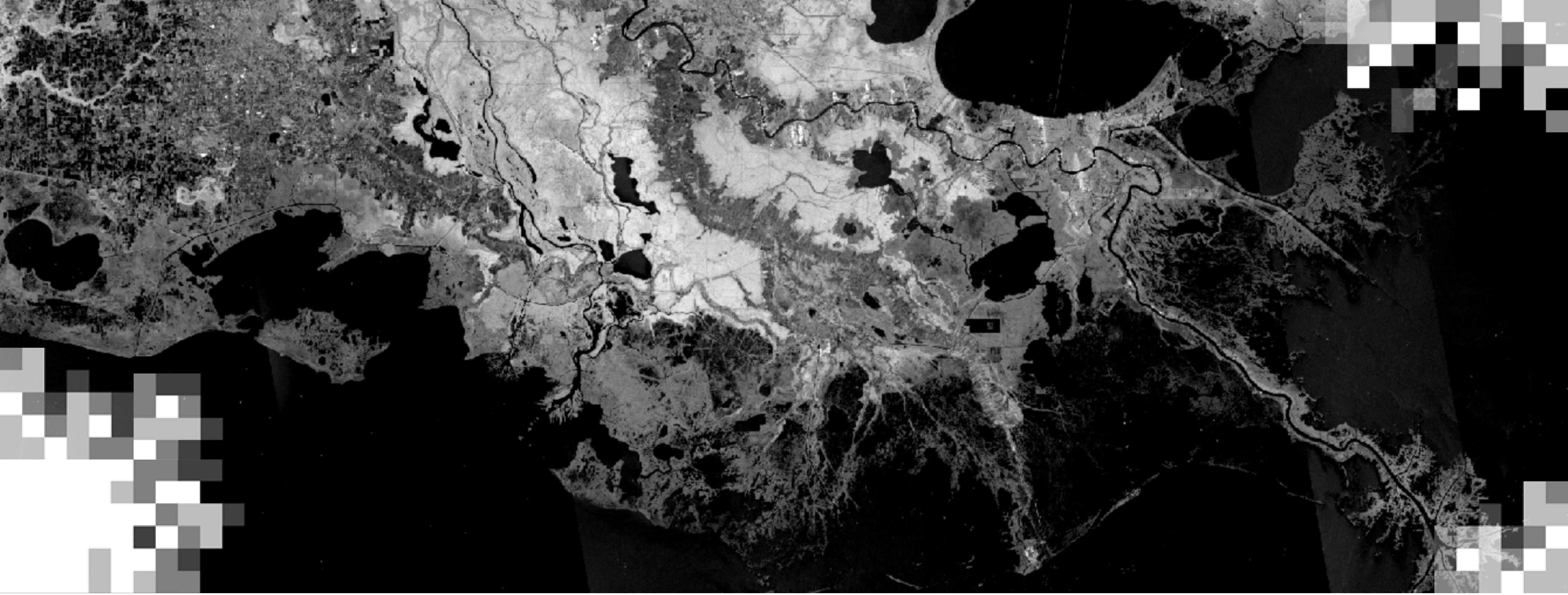

InSAR Applications

Some Examples of Deformation

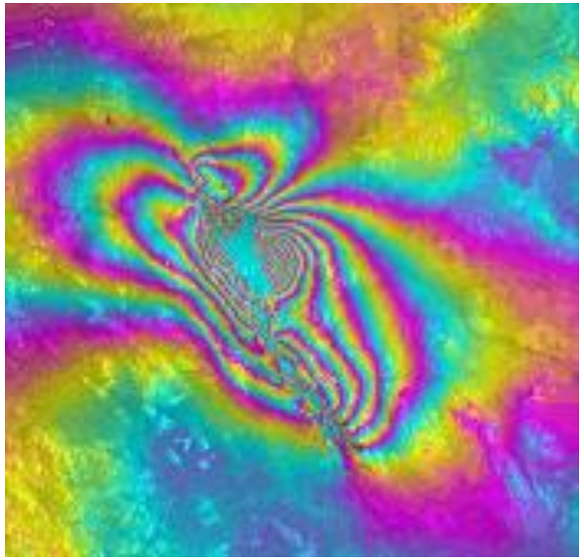

Hector Mine Earthquake

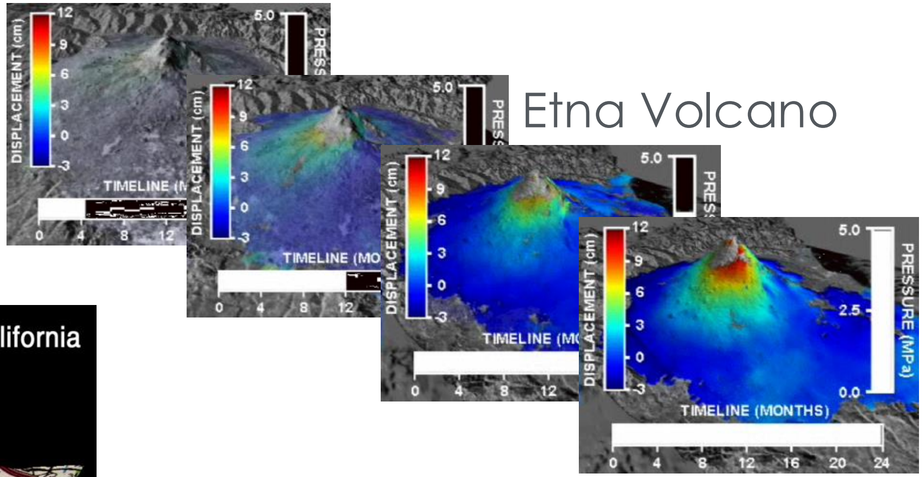

Etna Volcano

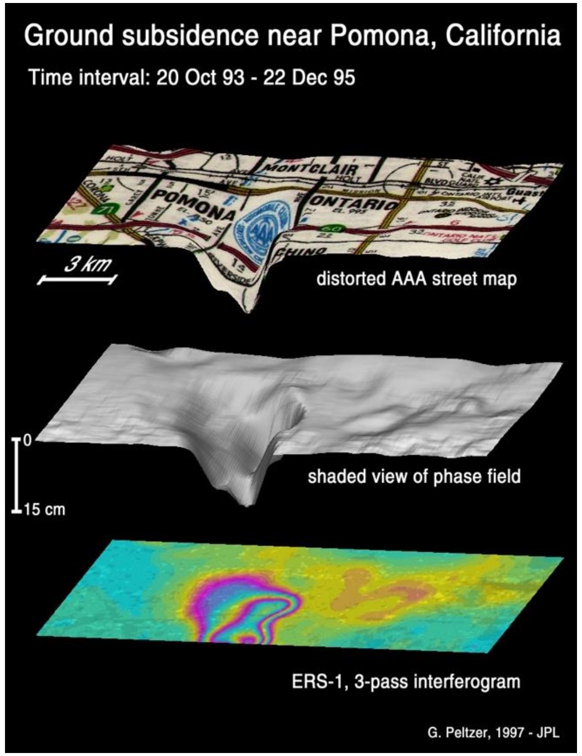

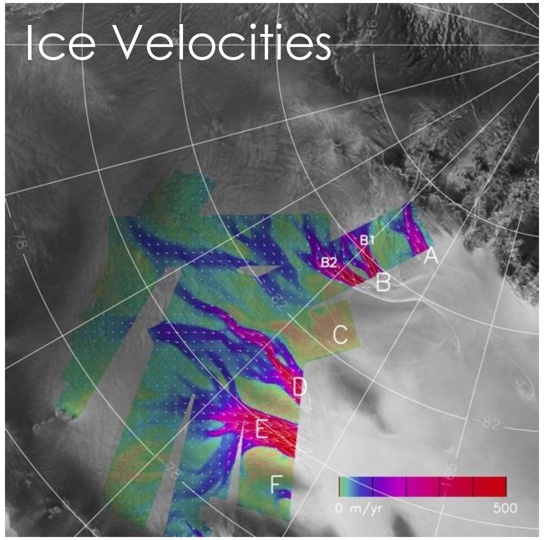

Joughin et al, 1999

Volcanoes of the Central Andes

- Map of deformation in and around volcanoes
- European ERS-1 and ERS-2 satellites (C-band)
- Some related to recent eruptions
- Others were not known to be active now
- Figure from M. Pritchard (now at Cornell)

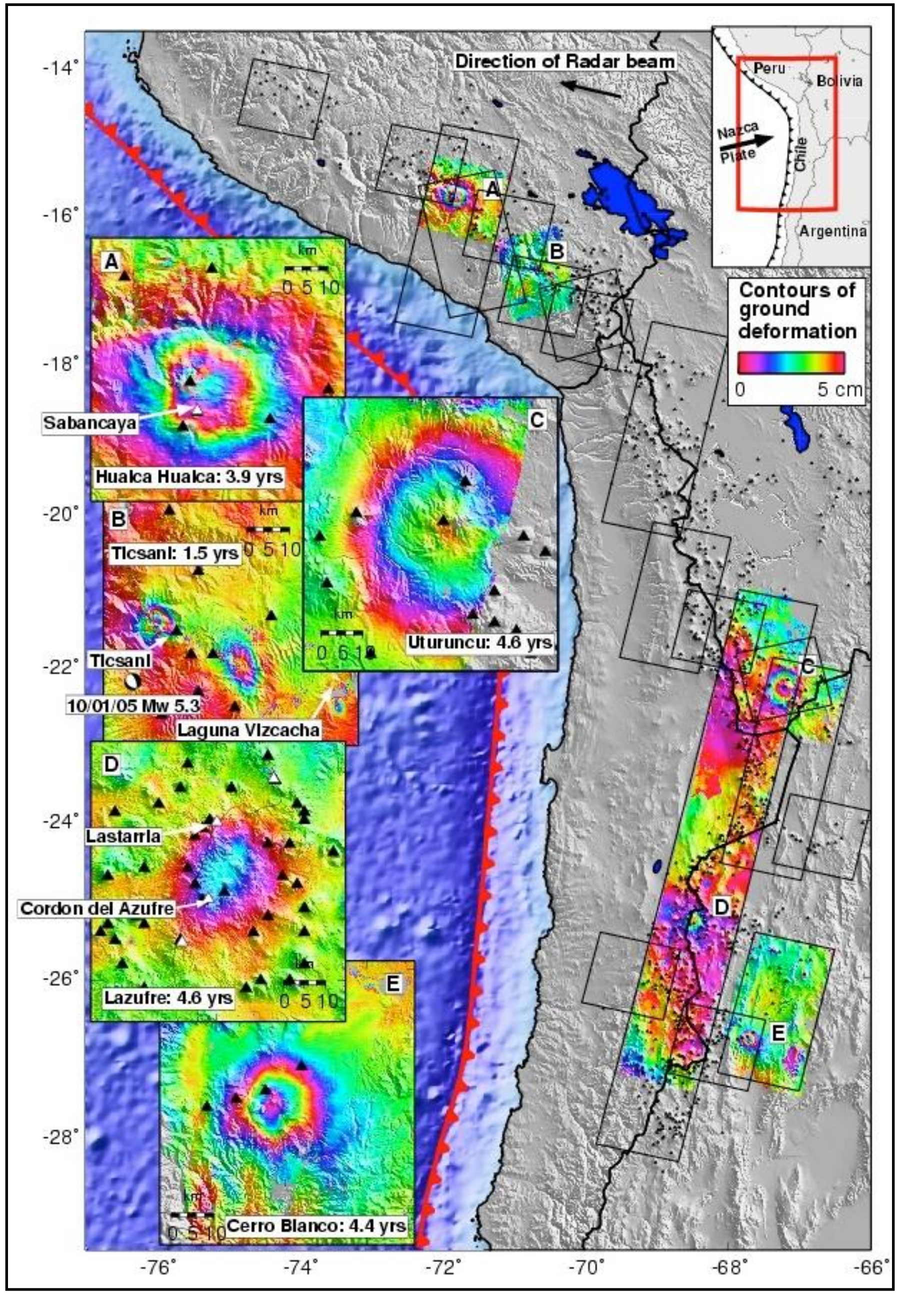

Afar Rift Dike Injection, Ethiopia

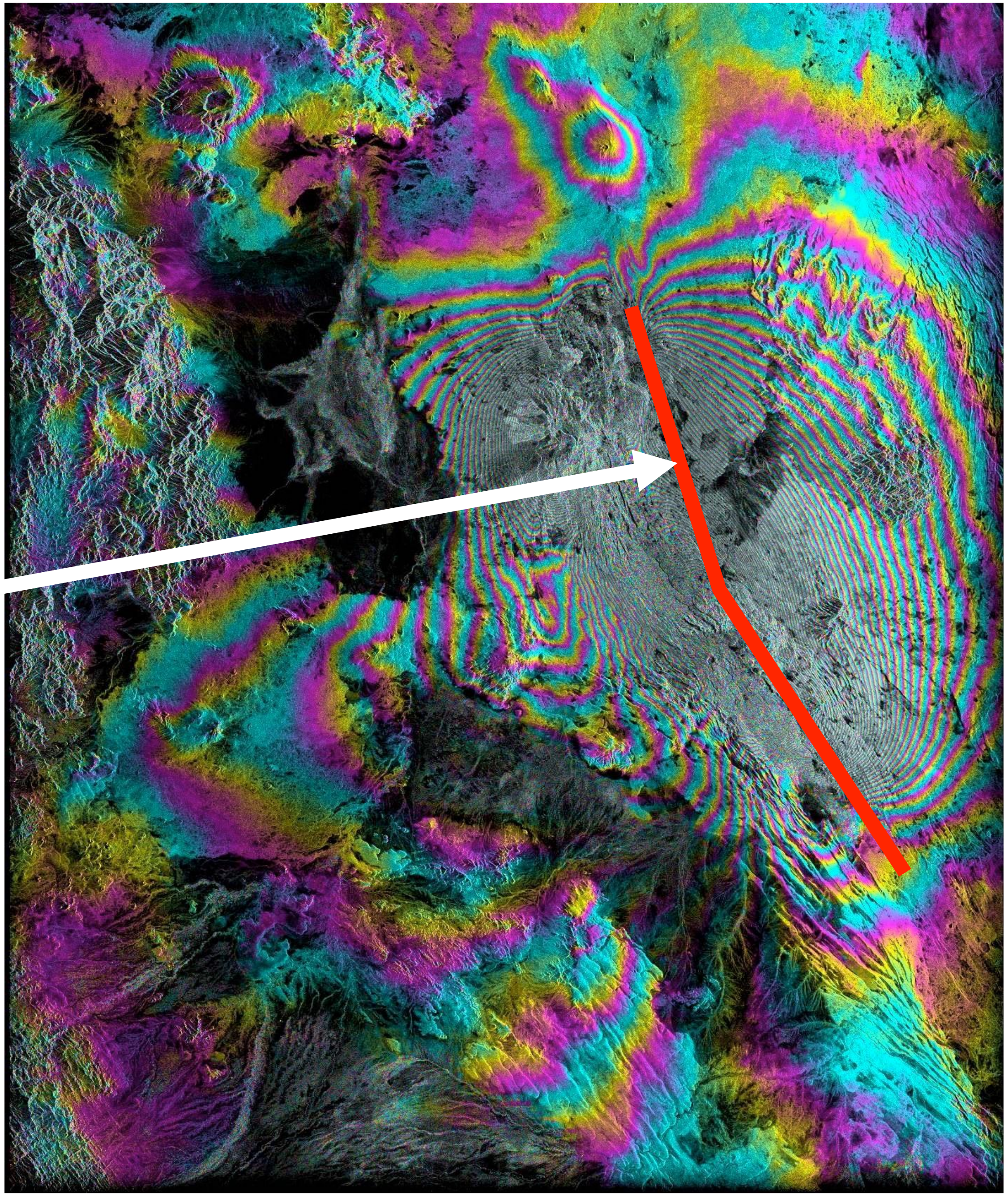

6 May – 28 Oct 2005; from Tim Wright, U. Leeds

2015 M7.8 Gorkha Earthquake in Nepal

- ALOS-2 ScanSAR interferogram
- Descending line-of-sight (LOS) perpendicular to horizontal
- InSAR phase only sees vertical component
- High Himalayas dropped down as much as 1.2 m
- Yue, H., et al. (2017), Depth varying rupture properties during the 2015 Mw 7.8 Gorkha (Nepal) earthquake, *Tectonophysics*, doi:10.1016/j.tecto.2016.07.005.

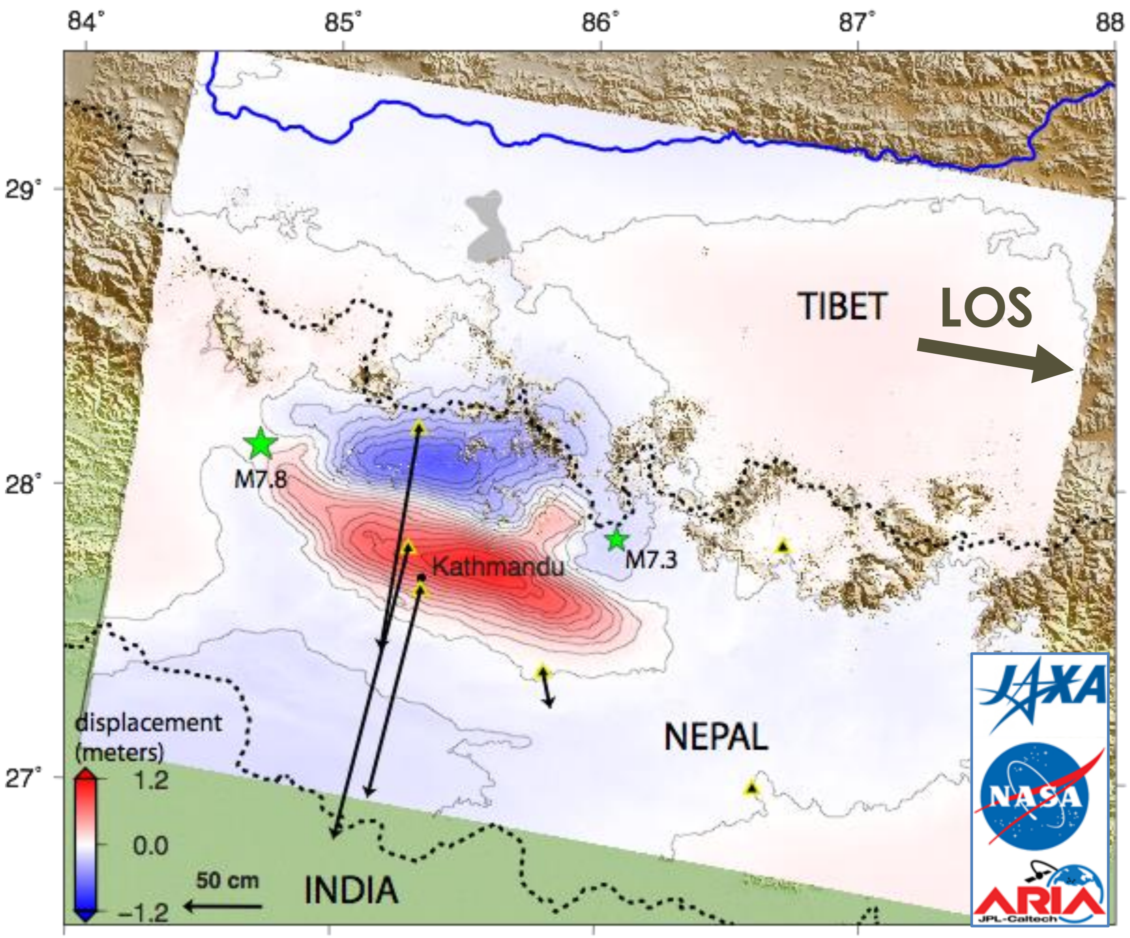

GPS data from Galetzka, J., et al. (2015), Slip pulse and resonance of the Kathmandu basin during the 2015 Gorkha earthquake, Nepal, *Science 349(6252), 1091-1095.*

Creep on the San Andreas Fault

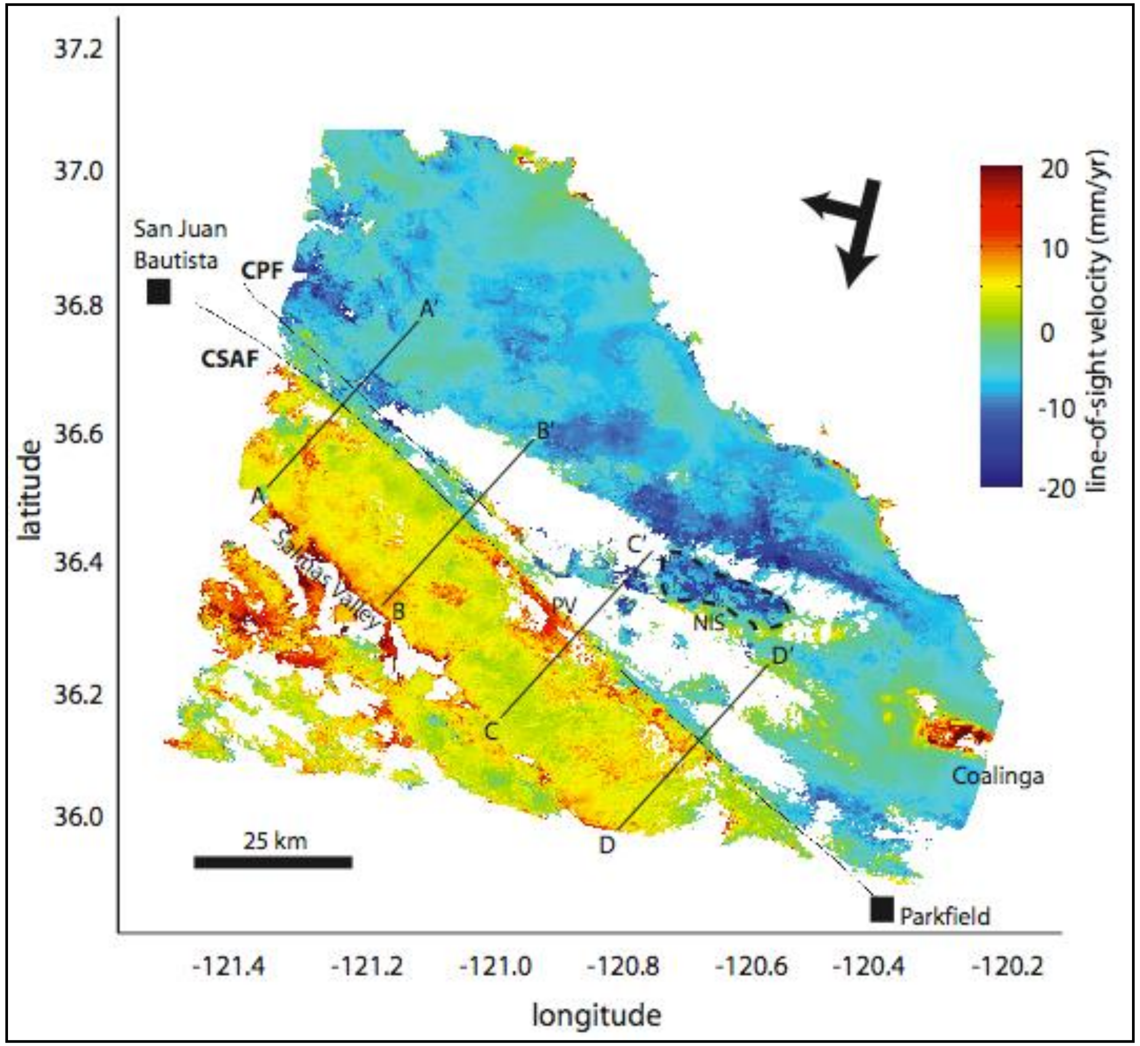

Stack of 12 ERS Interferograms Spanning May 1992-Jan 2001

Figures from Isabelle Ryder
UC Berkeley

Some of InSAR's Greatest Hits

The Ups and downs of Las Vegas (From Groundwater Pumping)

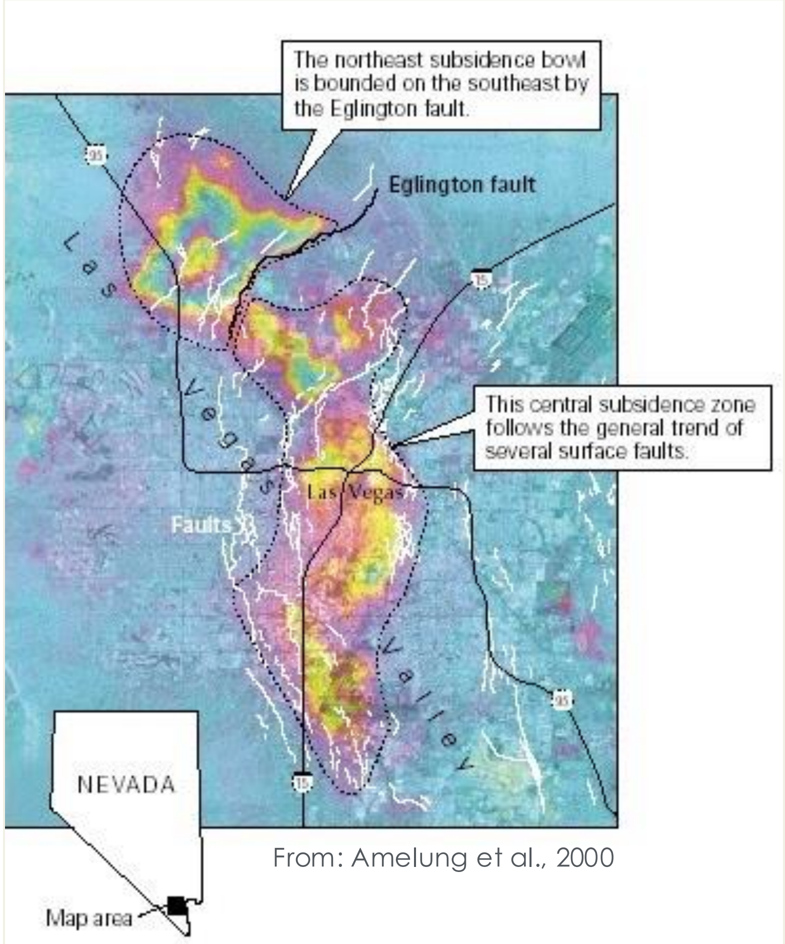

From: Amelung et al., 2000

Antarctica Ice Stream Velocities from InSAR/Feature Tracking

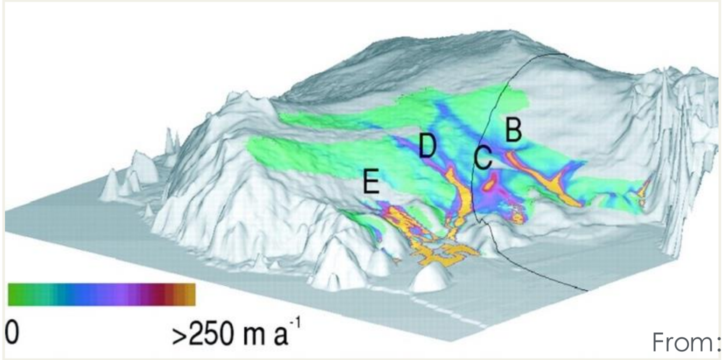

From: Bamber et al., 2000

Enhanced Oil Recovery Detected in the San Jorge Basin, Argentina

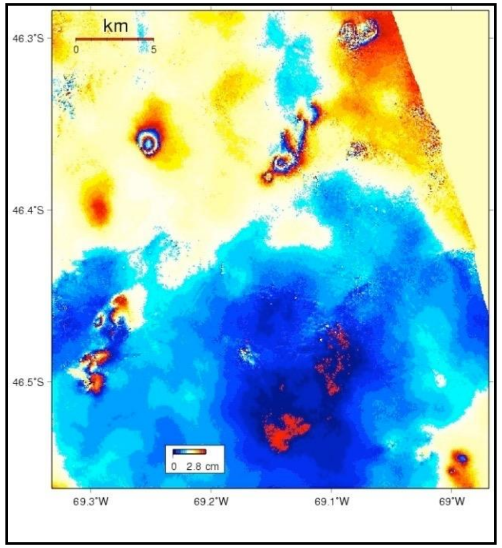

Envisat Interferogram Spans 2004-2006

Slide Modified from Matt Pritchard (Cornell)

Decorrelation Shows Surface Ruptures

2003 M6.5 Bam Earthquake in Iran

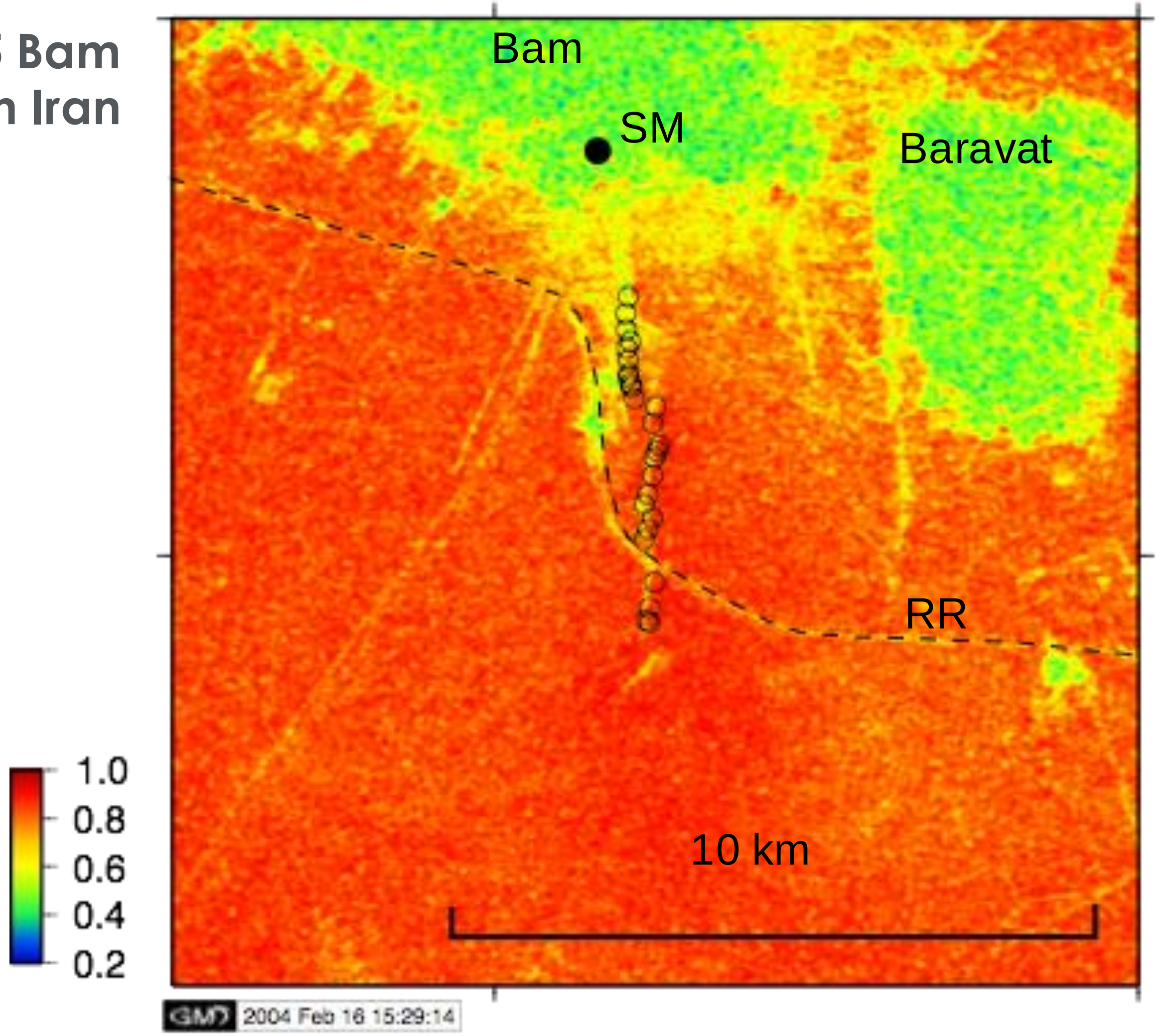

35 days
2003/12/3 – 2004/1/7

Envisat
Descending track
Bperp 580 m

Fielding, E. J., M. Talebian, P. A. Rosen, H. Nazari, J. A. Jackson, M. Ghorashi, and R. Walker (2005), Surface ruptures and building damage of the 2003 Bam, Iran, earthquake mapped by satellite synthetic aperture radar interferometric correlation, *J. Geophys. Res.*, *110*(B3), B03302, doi:10.1029/2004JB003299.

Correlation Change

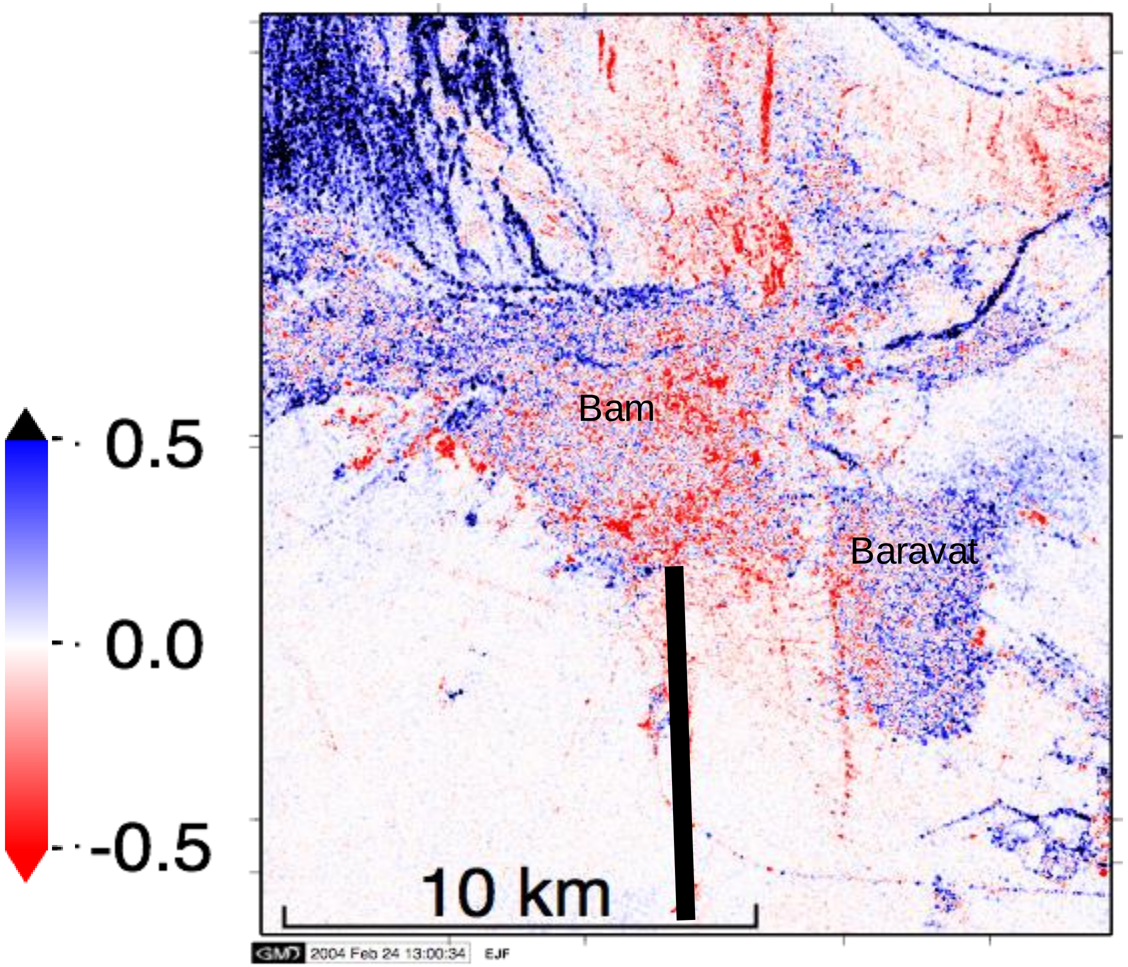

Co-Seismic Correlation Minus Pre-Seismic Correlation

Red is co-Seismic decorrelation

Landslide Motion

Combination of four NASA UAVSAR InSAR flight lines

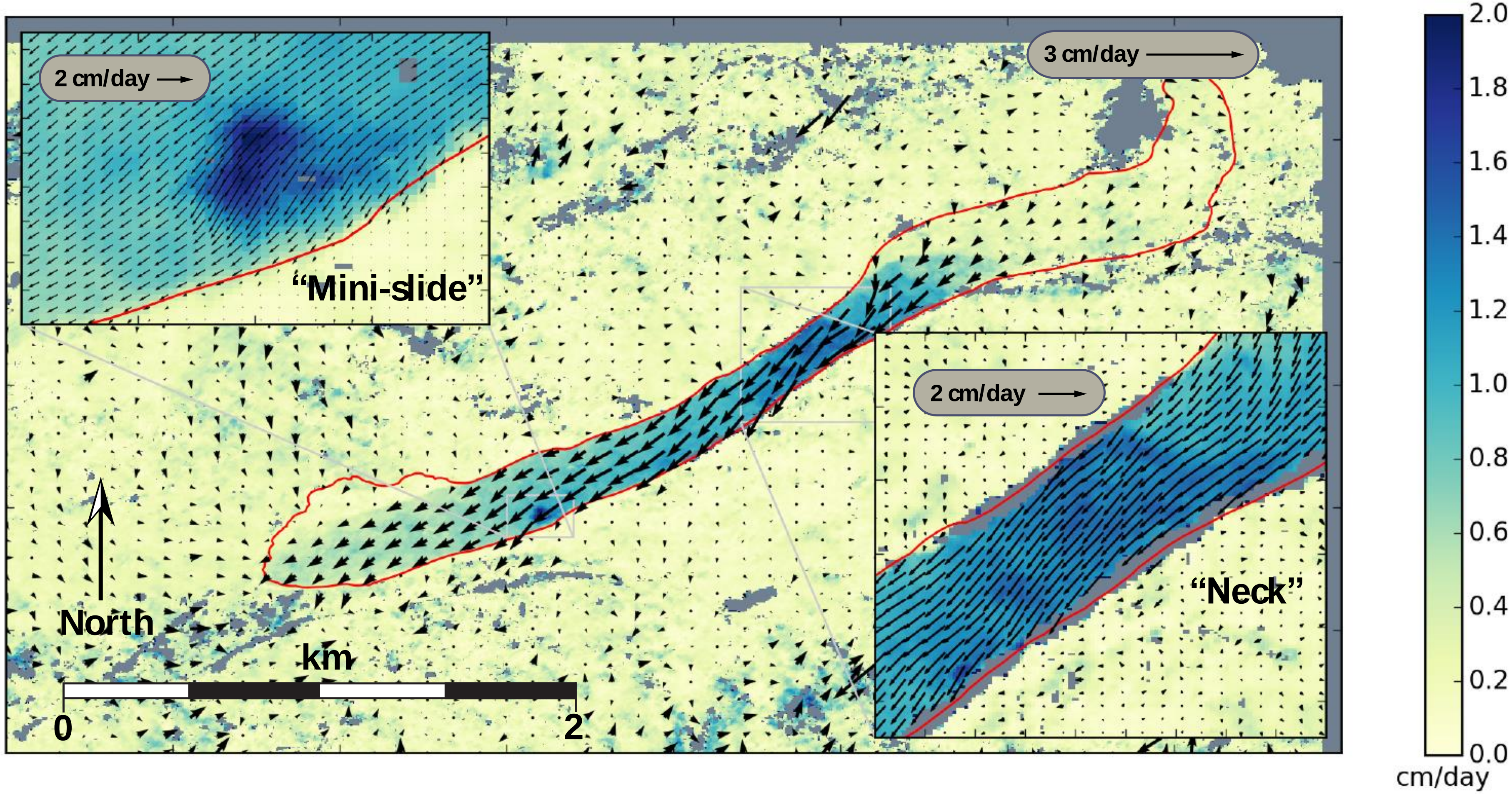

Delbridge, B. G., R. Bürgmann, E. Fielding, S. Hensley, and W. H. Schulz (2016), Three-dimensional surface deformation derived from airborne interferometric UAVSAR: Application to the Slumgullion Landslide, J. Geophys. Res. Solid Earth, 121(5), 3951--3977, doi:10.1002/2015JB012559.

NASA-ISRO SAR Mission (NISAR)

- High spatial resolution with frequent revisit time
- Global land coverage
- Planned Launch Date: Early 2025
- Dual Frequency L- and S-band SAR
  - L-band SAR from NASA and S-band SAR from ISRO
- 3 years science operations (5+ years consumables)
- All science data will be made available free and open
- https://nisar.jpl.nasa.gov

Slide Modified from Paul Rosen (JPL)

NISAR Science Observation Summary

NISAR Uniquely Captures the Earth in Motion

NISAR Characteristic:	Would Enable:
L-Band (24 cm Wavelength)	Low Temporal Decorrelation and Foliage Penetration
S-Band (9.4 cm Wavelength)	Sensitivity to Light Vegetation
SweepSAR Technique with Imaging Swath > 240 km	Global Data Collection
Polarimetry (Single/Dual/Quad)	Surface Characterization and Biomass Estimation
12-Day Exact Repeat	Rapid Sampling
3–10 Meters Mode-Dependent SAR Resolution	Small-Scale Observations
3 yrs (NASA)/5 yrs (ISRO) Science Operations	Time-Series Analysis
Pointing Control < 273 Arcseconds	Deformation Interferometry
Orbit Control < 500 meters	Deformation Interferometry
> 10% (S)/50% (L) Observation Duty Cycle	Complete Land/Ice Coverage
Left-Only Pointing (Left/Right Capability)	Uninterrupted Time-Series Rely on Sentinel-1 for Arctic

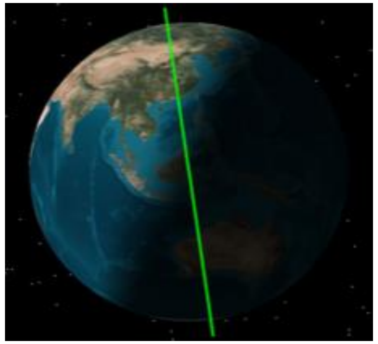

6 AM/6 PM

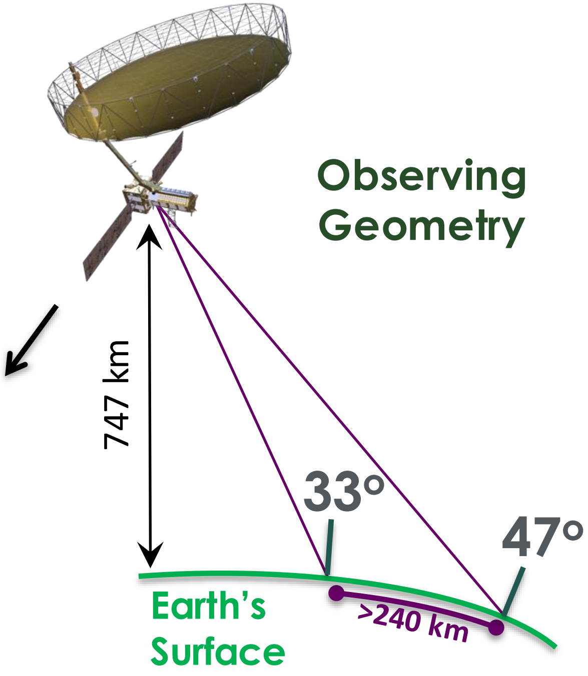

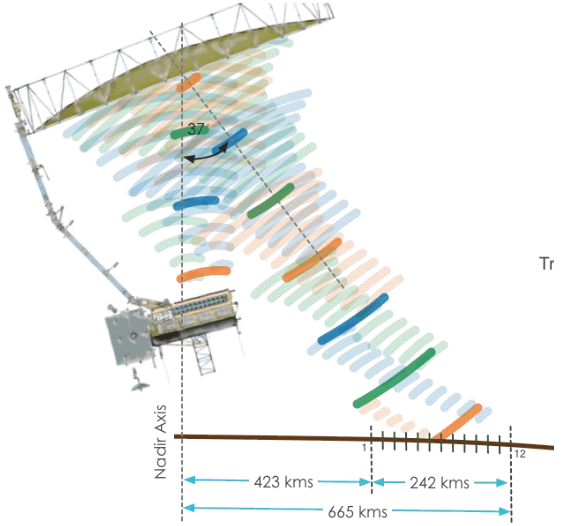

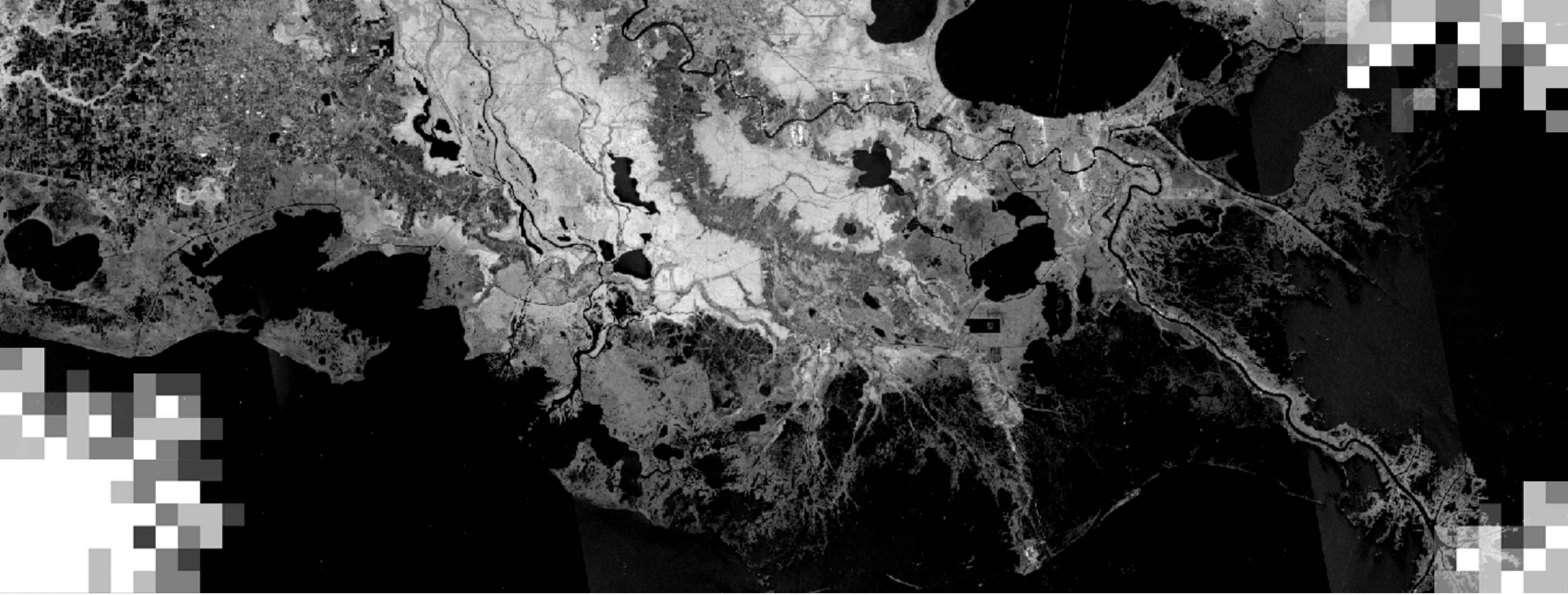

InSAR Processing

Demonstration with SAR from Copernicus Sentinel-1

- Sentinel-1 SAR Global Coverage
- European Union Copernicus Sentinel-1 SAR satellites have been operating since late 2014.
- Data is free, open, and acquired globally with varying temporal frequency.
- Sentinel-1A, launched in 2014, started regular operations in October 2014.
- Sentinel-1B launched and started operations in 2016. Anomaly 23 December 2021 ended SAR operations.
- Sentinel-1C ready for launch, now planned for 3 December 2024.
- Sentinel-1D nearly ready to be launched, about 6 months after Sentinel-1C.
- All Sentinel-1 satellites are in 12-day repeating orbits, using C-band SAR.
- Sentinel-1A and -1B flew over each track 6 days apart, enabling 6-day repeats over Europe and selected other areas.

Sentinel-1 TOPS Mode

- Sentinel-1 uses TOPS over almost all land.
- TOPS is "Terrain Observation by Progressive Scans".
- Three sub-swaths.
- Bursts in each subswath cover about 90 by 20 km.

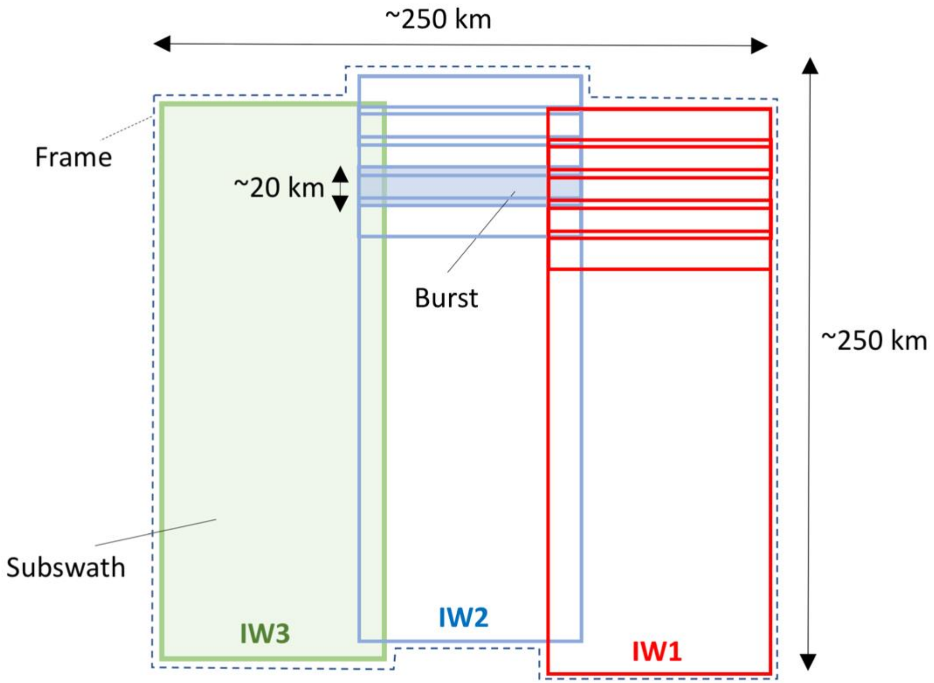

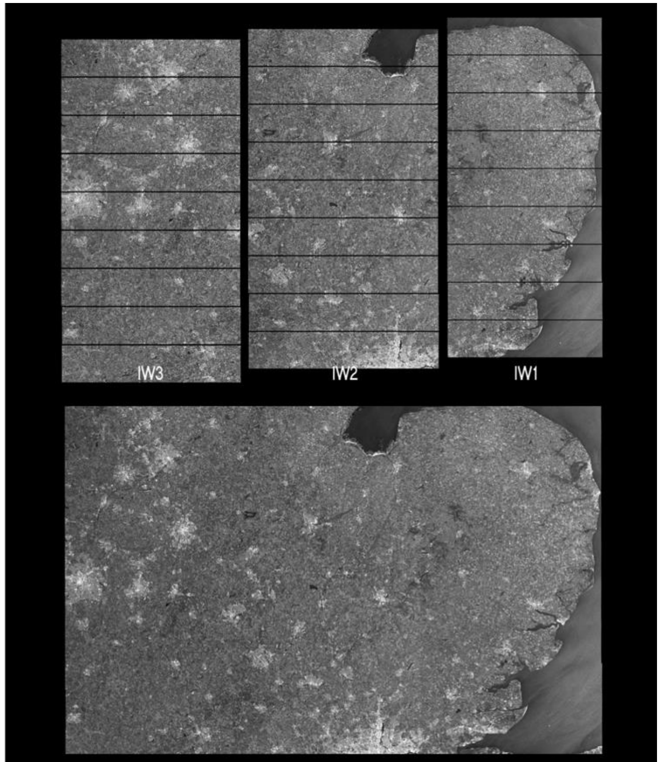

Slide Modified from Heresh Fattahi (JPL)

Sentinel-1 SAR Data Products

- ESA and NASA processing
- ESA processes Sentinel-1 raw, single-look complex (SLC), and geocoded ground range detected (GRD) products for Copernicus
- ESA products are for slices of the satellite track that are not always in the same location
- Raw, SLC, and GRD archived at Copernicus DataSpace
- NASA Alaska Satellite Facility (ASF) Distributed Active Archive Center (DAAC) mirrors Copernicus Sentinel-1 archive
- ASF DAAC provides access to individual bursts as SLC products in radar coordinates.
- NASA JPL OPERA project processes SLC bursts to co-registered SLC (S1 CSLC) products in geocoded coordinates for North America, archived at ASF
- NASA JPL ARIA project process adjusted selected pairs of dates to geocoded unwrapped interferograms (S1-GUNW), archived at ASF

NISAR InSAR Data Products

- Planned products from NISAR will cover standard frames and be at the ASF DAAC.
- **Radar Coordinates Wrapped Interferograms (RIFG)** in areas of ice sheets
- **Geocoded Single-Look Complex (GSLC)**, very similar to OPERA S1-CSLC
- **Geocoded Unwrapped Interferograms (GUNW)**, very similar to ARIA S1-GUNW
- **Radar Coordinates SLC (RSLC)**

Making an Interferogram from CSLC Products

- Using a Jupyter Notebook
- ARSET demonstration notebooks available from: https://github.com/EJFielding/ARSET_notebooks
- ARSET_notebooks/Map_Hawaii_Deformation_LavaFlow_using_CSLC-S1.ipynb downloads CSLC products and makes interferogram and coherence maps.
- Additional notebooks available from: https://github.com/OPERA-Cal-Val/OPERA_Applications

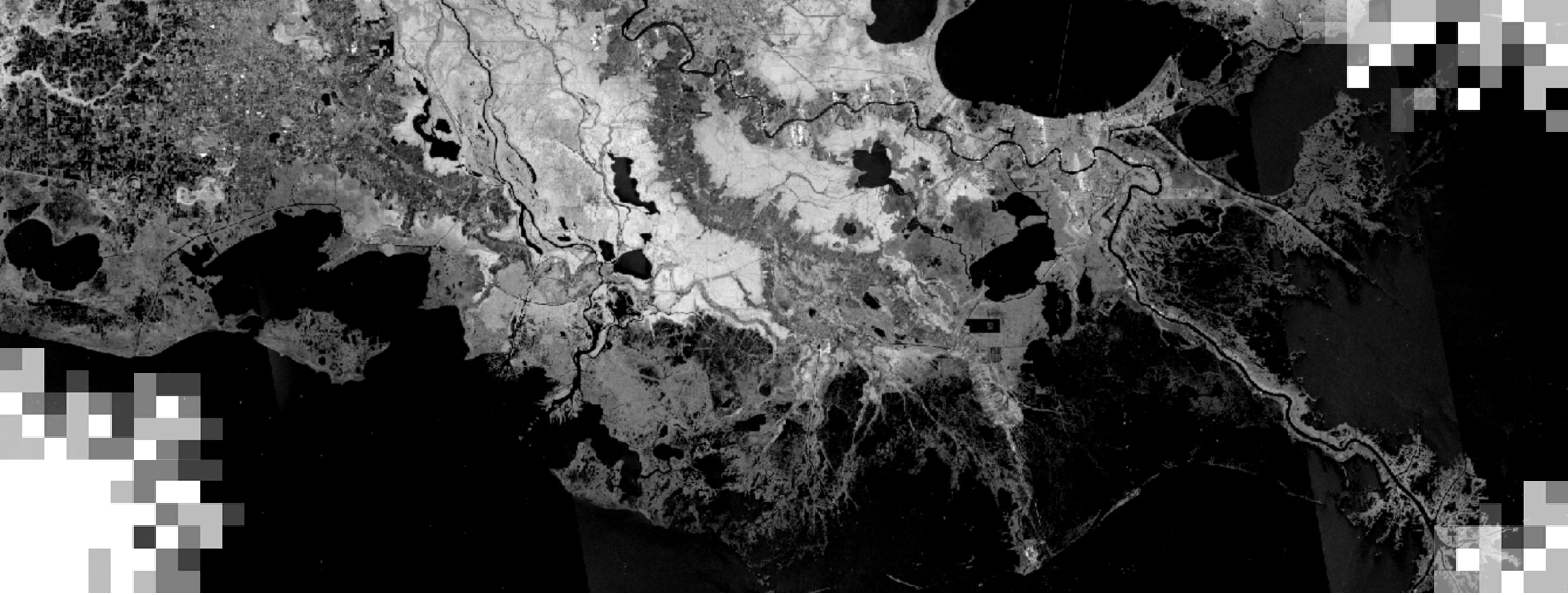

Searching SAR Interferometry Data

Searching for OPERA Sentinel-1 CSLC for Interferometry

1. Go to the Alaska Satellite Facility Search Portal: https://search.asf.alaska.edu/#/.
2. Find the Big Island of Hawaii and draw a box around Mauna Loa.
3. Set Start and End dates (Nov. 15 to Dec. 15, 2022) of interest (2022 Mauna Loa Eruption).
4. Choose Dataset (OPERA-S1).
5. Click **Search**.
6. Select Granule: `OPERA_L2_CSLC-S1_T087-185682-IW2_20221204T161649Z_20240504T113337Z_S1A_VV_v1.1` (Track 87 burstID 185682).
7. This is the OPERA Sentinel-1 Co-registered Single Look Complex (CSLC) (252 MB) Product acquired on 2022/12/04.
8. We will download data with Jupyter Notebook later.
9. See Part 3 of this series for more details on ASF data searching.

Searching for OPERA Sentinel-1 CSLC for Interferometry

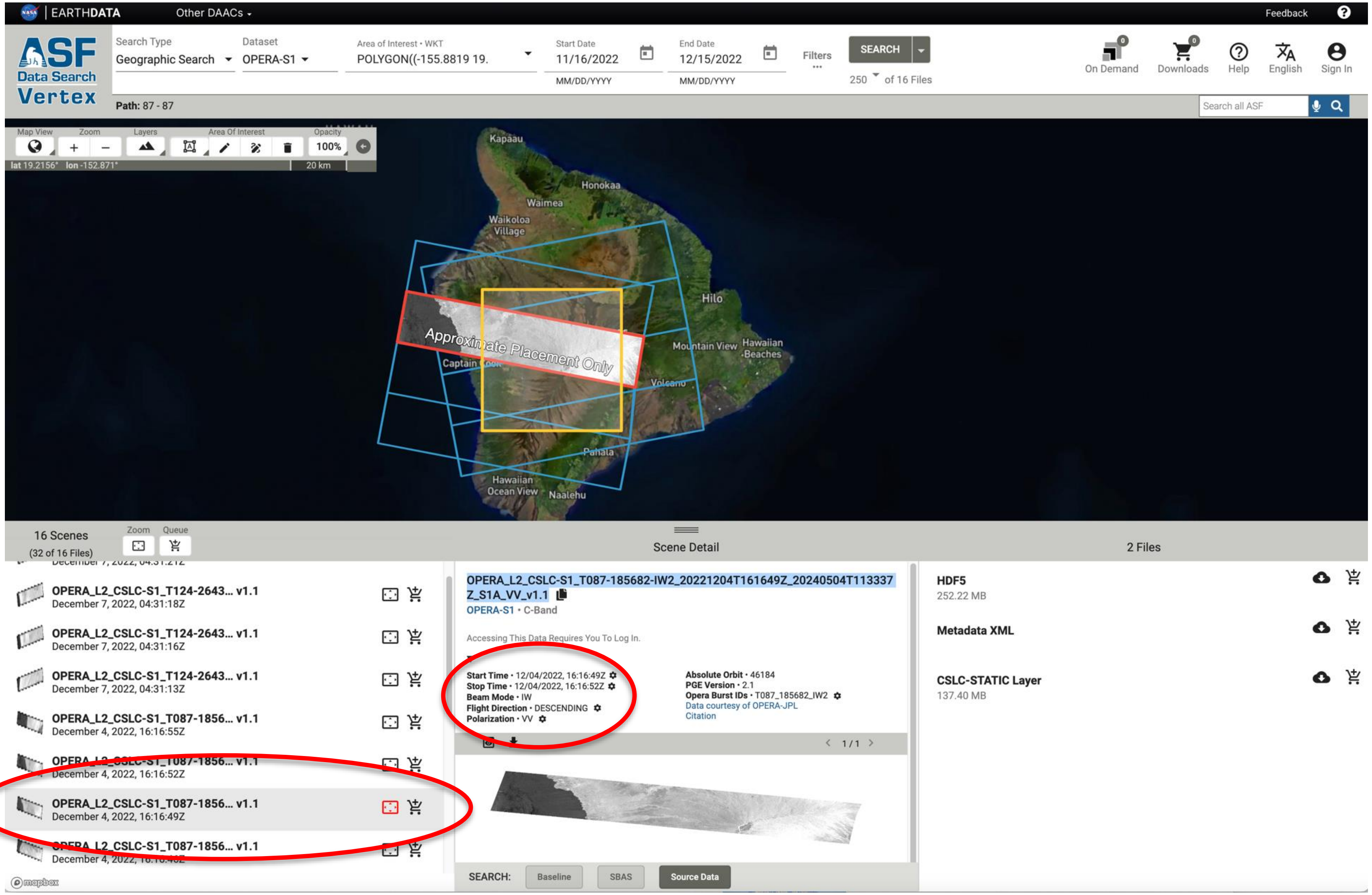

- Selected CSLC is from track 87 and is a descending track.
- Date 20221204 is the first S1 after the eruption started on November 27.

Searching for ARIA Sentinel-1 GUNW Interferograms

- Alternative way to get pre-processed interferograms

1. Go to the Alaska Satellite Facility Search Portal: https://search.asf.alaska.edu/#/ (same as before).
2. Keep or redraw a box around Mauna Loa.
3. Keep Start and End dates (Nov. 15 to Dec. 15, 2022) of interest (2022 Mauna Loa Eruption).
4. Choose Dataset (ARIA S1 GUNW).
5. Click **Search**.
6. Select Granule: `S1-GUNW-D-R-087-tops-20221204_20221122-161643-00157W_00019N-PP-0316-v3_0_1` (Track 87).
7. This is the ARIA Sentinel-1 Geocoded Unwrapped interferogram (GUNW) (107 MB) from data acquired on 2022/11/22 and 2022/12/04.
8. See 2023 ARSET InSAR training for demonstration of use of GUNW files for time-series analysis.

Searching for OPERA Sentinel-1 CSLC for Interferometry

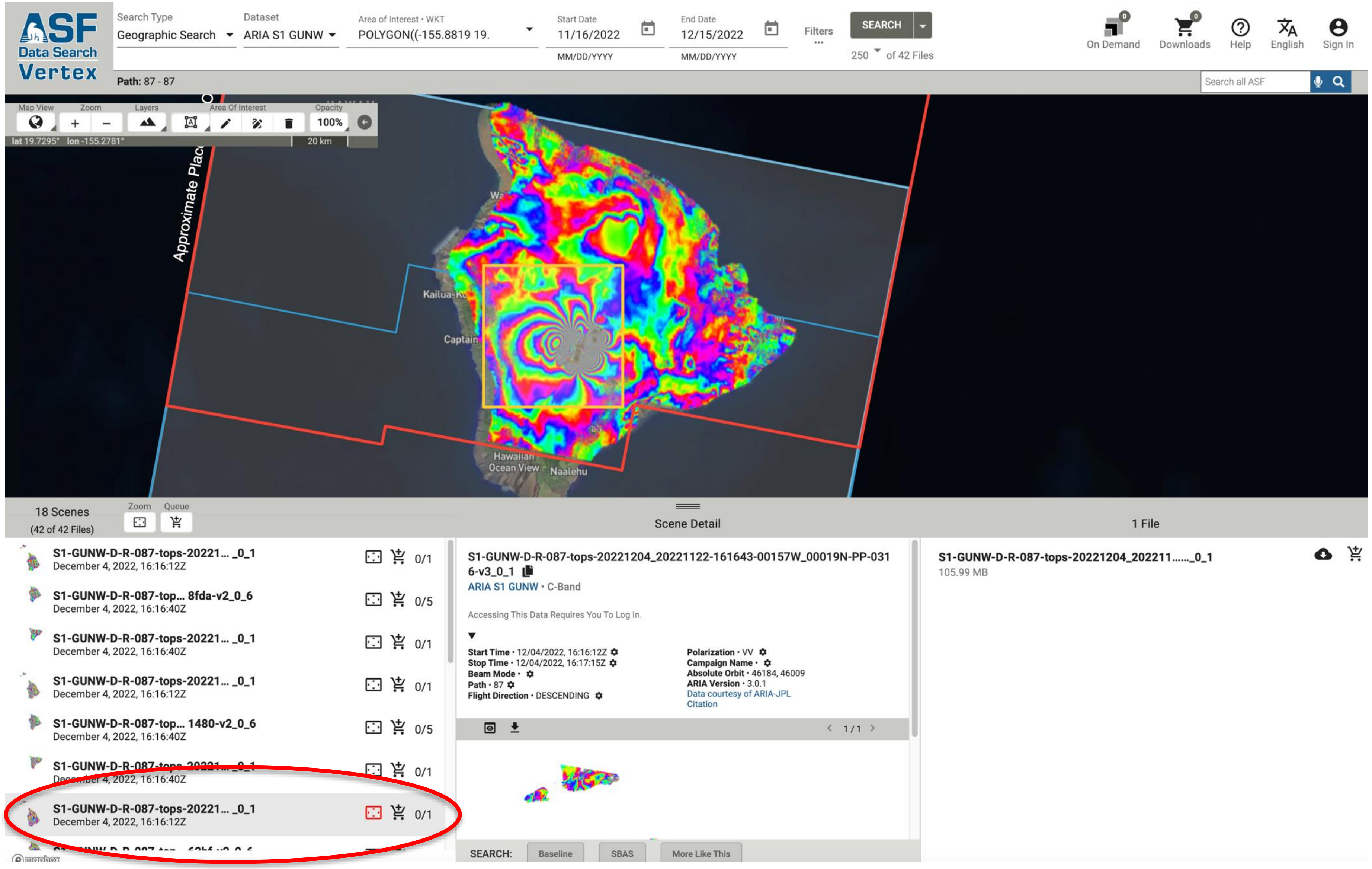

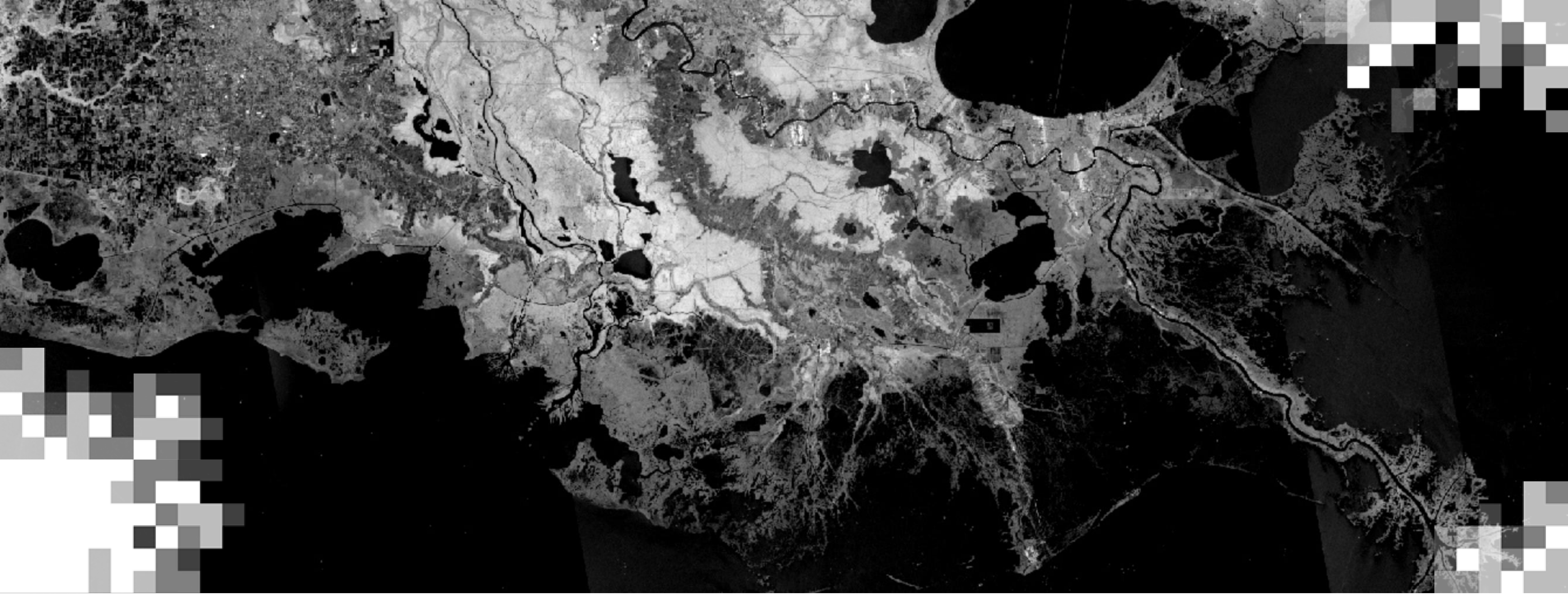

Processing CSLC or GSLC

Interferogram Formation GSLC or CSLC

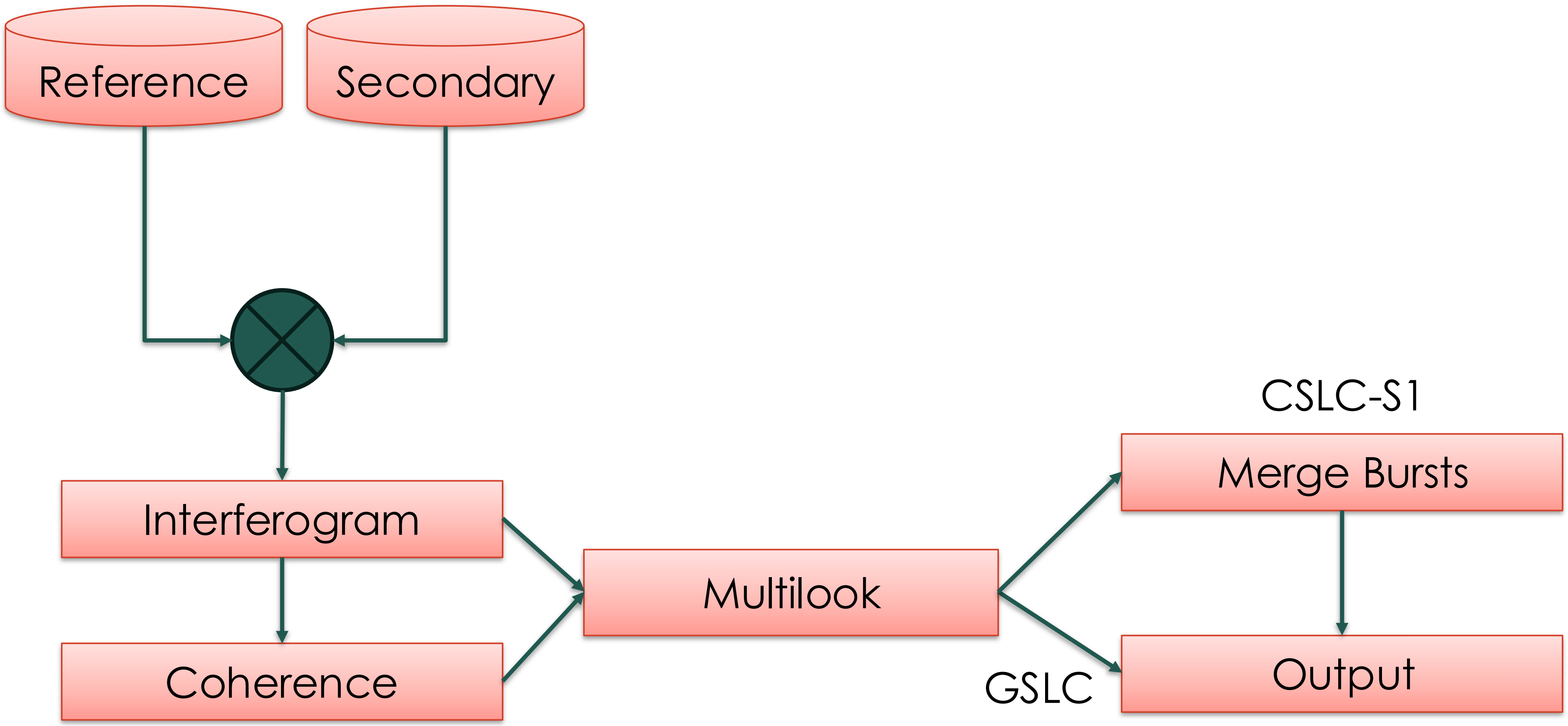

Interferogram Demonstration with S1-CSLC Data over Hawaii

(1) Download OPERA CSLC bursts

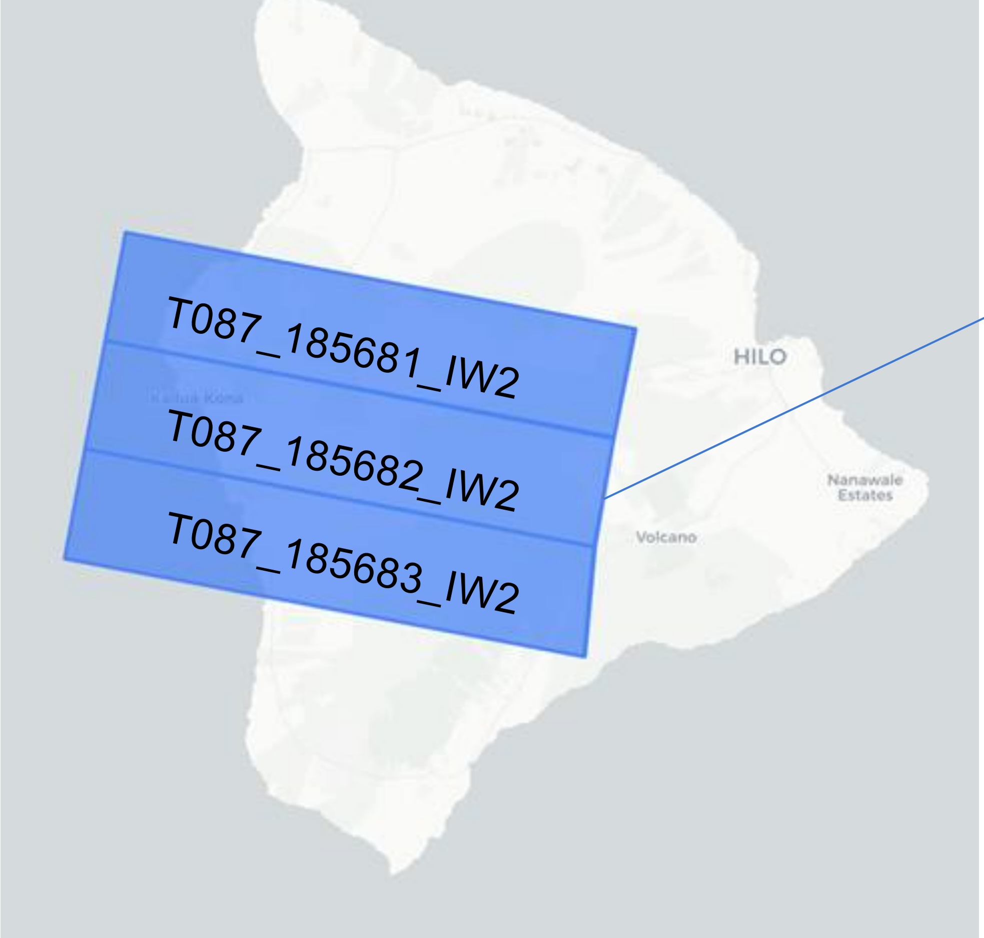

(2) Compute *burst-wise* interferogram and coherence

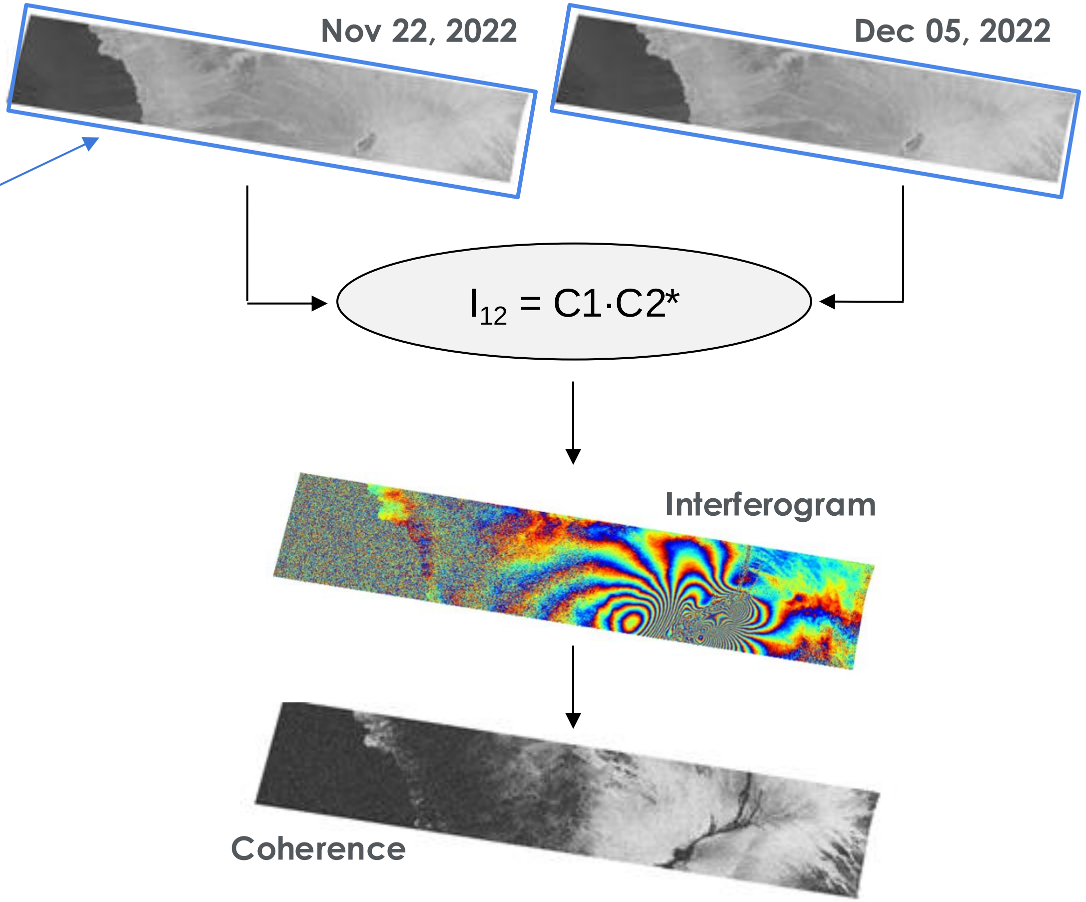

Hawaii Interferogram Visualization

(3) Stitch, save, and plot/visualize

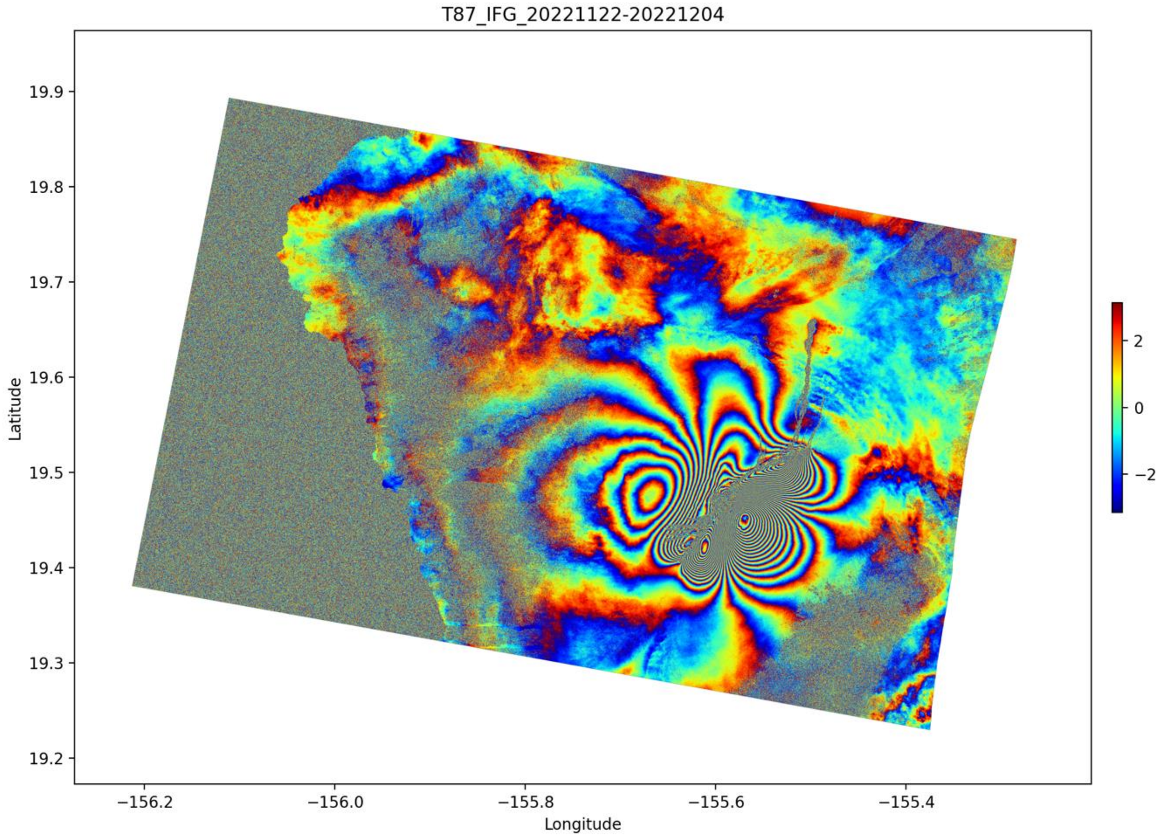

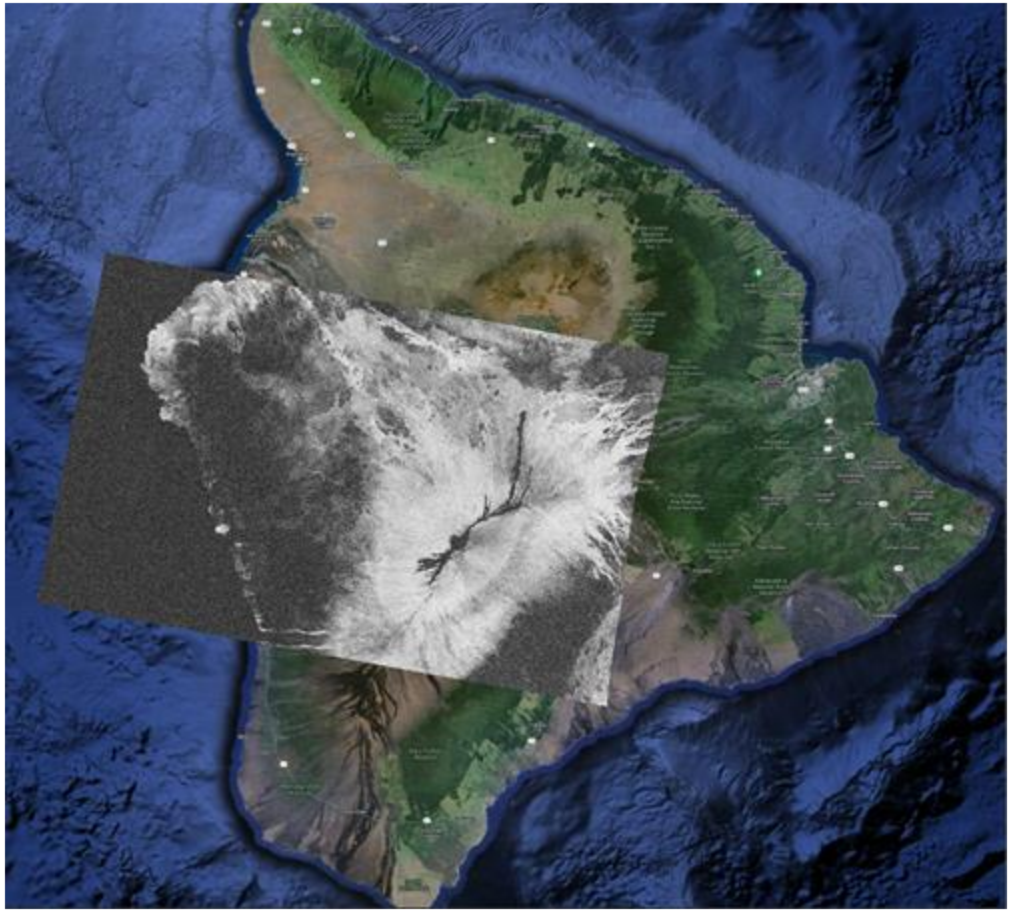

Slide Modified from M. Grace Bato (JPL)

Summary

- SAR interferometry (InSAR) measures distance from satellite to ground with high precision by using phase of reflected radar signals.
- Coherence of InSAR phase is sensitive measure of surface or surface cover stability at radar wavelength scale.
- Phase cycles in a repeat-pass interferogram show change in distance to ground by half the radar wavelength, 2.8 cm for Sentinel-1 and 12 cm for NISAR.
- New pre-processed InSAR products enable user analysis of interferograms with few additional steps.
- InSAR measurements of surface motion are useful for variety of geological processes, some hydrological processes, dynamics of glaciers, and other effects that displace surface or large structures.

Homework and Certificates

- **Homework:**
  - One homework assignment
  - Opens on 11/20/2024
  - Access from the training webpage
  - Answers must be submitted via Google Forms
  - **Due by 12/04/2024**

- **Certificate of Completion:**
  - Attend all three live webinars (attendance is recorded automatically)
  - Complete the homework assignment by the deadline
  - You will receive a certificate via email approximately two months after completion of the course.

Contact Information

Trainers:

- Dr. Eric Fielding
  - eric.j.fielding@jpl.nasa.gov

- ARSET Website
- Follow us on Twitter!
  - @NASAARSET
- ARSET YouTube

Visit our Sister Programs:

- DEVELOP
- SERVIR

Thank You!